Université de Liège
Faculté des Sciences Appliquées

Integration of Photovoltaic Panels Into Low-voltage Distribution Networks

Travail de fin d'études réalisé en vue de l'obtention
du grade de master Ingénieur Civil en Electricité par

Olivier Frédéric

sous la direction du
Pr Dr Damien Ernst

Année académique 2012–2013

Université de Liège
Faculté des Sciences Appliquées

Integration of Photovoltaic Panels Into Low-voltage Distribution Networks

Travail de fin d'études réalisé en vue de l'obtention
du grade de master Ingénieur Civil en Electricité par

Olivier Frédéric

sous la direction du
Pr Dr Damien Ernst

Année académique 2012–2013

Abstract

Integration of Photovoltaic Panels Into Low-voltage Distribution Networks

Olivier Frédéric

Electrical engineering
University of Liège
Academic year 2012–2013

We address in this thesis the problem of overvoltages caused by photovoltaic (PV) panels in low-voltage networks. As a solution to this problem, we propose new active network management schemes. They work by modulating in an ad-hoc way the power injected by the PV inverters into the low-voltage network. Two types of control schemes are studied: centralized ones and distributed ones. The centralized schemes compute the modulation orders by exploiting an optimal power flow formulation of the problem. The distributed schemes are based on simple control logics implemented in the inverters and using only local information. Henceforth, they are less expensive to build than centralized ones. Both types of schemes are tested on a simple test network. The simulation results show that they are indeed able to control the voltages so that they stay within their limits. Moreover, the distributed schemes are shown to perform almost as well as the centralized ones, when using as performance metric the amount of energy curtailed on the PV installations.

Acknowledgements

First of all, I would like to express my gratitude to my supervisor Prof. Dr. Damien Ernst for his guidance, support and great availability.

I also would like to thank Prof. Dr. Thierry Van Cutsem for many relevant remarks concerning the work reported in this thesis.

I am also grateful to all the Professors of the Faculty of Applied Sciences of the ULg for the excellent training they offered me over these last five years.

Finally, I would like to thank my parents for their love, their support as well as for teaching me the value of education.

Contents

Chapter 1

Introduction

The run towards renewable energy sources has started. Everywhere around the world, we see governments taking actions to favor the development of green energy. Thanks to generous subsidies, solar power production has taken off in many European countries and, in particular, in Belgium. Indeed, there are now more than 2 GW of photovoltaic panels installed in our country. These latter years, it has been observed that PV panels installed on houses were causing significant problems to the low-voltage network to which they were connected. More specifically, they are leading to unacceptable voltage rises that significantly endanger the security of the electrical network. By way of example, in Wallonia, voltages of more than 290 V have been observed in low-voltage networks to which PV panels were connected, which is unacceptable. Additionally, if strategies are not rapidly developed to address these overvoltage problems caused by PV installations, it is very likely that it will slow down considerably the development of solar power production.

Command structure of power electricity networks

Before further explaining the strategies studied in this master thesis for mitigating the voltage problems caused by PV panels, we discuss the existing structure of the electricity grid and the basic strategies put in place for its operation. The electricity grid, as we know it now, is composed of two main layers. The top-layer is made of a transmission network and the bottom layer of distribution networks. The transmission network, as its name suggests, is transmitting electricity over long distances at high voltages. The entity in charge of operating the transmission network is the

Transmission System Operator, or TSO in short. Distribution networks, which are operated by Distribution System Operators (DSO) connect the transmission network to the end customers.[1] In Wallonia, they are generally operated at voltages ranging from 230 V till 30 kV while transmission networks are operated at voltages starting from 70 kV and up to 380 kV. TSOs usually have in their possession different detailed models of their networks that they use on a daily basis for operating their systems. For example,

- They use these models in combination with real-time measurements to estimate the state of the system.
- They run load-flows based on these models to check for example (i) whether in the aftermath of a contingency, lines or transformers will exceed their current limits (ii) whether they can indeed authorize the production plans of generation companies.
- With detailed dynamical models of their system, they run dynamical simulations to check whether the system is sufficiently secure with respect to more complex instability phenomena, such as loss of synchronism phenomena or voltage instability.

Distribution network operators usually do not rely on models for running on a daily basis their system. Indeed, they rather rely on the so-called *fit and forget* doctrine for daily operation. The key idea behind this doctrine is to *fit* the distribution system in such a way that it can run smoothly with any control actions, i.e. that you can *forget* its existence once it is built. As a consequence, there was very little need for even modeling their network.

Active network management as an alternative to the fit and forget doctrine

With the rapid development of renewable energy sources, it becomes however more and more costly to enforce this doctrine and there is a push for managing the distribution networks in a smarter way, rather than relying on hefty investments. This has led to the recent development of *Active Network Management* (ANM) schemes for operating distribution networks. These schemes are usually centralized control schemes that exploit a model of the distribution network to modulate in a smart way the power injected or withdrawn from the distribution networks to avoid congestion

[1] Note that large industrial loads are sometimes directly connected to the transmission network.

or voltage problems. They are usually developed on the basis of the Optimal Power Flow (OPF) problem. Here is a non-exhaustive list of references describing ANM schemes based on an OPF-type formulation: [5], [7], [12], [13], [14] and [15]. In this master thesis, we will design ANM schemes for addressing the voltage problems caused by PV panels in the low-voltage distribution network.

On the need for model-free active network management schemes for integrating PV panels into the low-voltage network

However, we will not solely focus on centralized schemes based on an OPF-type formulation of the problem. Indeed, we will also propose distributed control schemes that are much simpler and less expensive to build. While our centralized control schemes rely on a potentially costly communication infrastructure and on a detailed model of the low-voltage network that may be difficult to get, our distributed control schemes work by implementing simple control logics on the inverters. Those logics use only local information. We remind that the inverters are the devices connecting the PV panels to the low-voltage network by transforming the Direct Current (DC) they produce into Alternative Current (AC).

Organization of the manuscript

This master thesis is organized as follows. In Chapter 2, we will present the low-voltage network that will be used throughout the whole manuscript for testing our control schemes. This chapter will also report on simulation results showing that this test network may be prone to overvoltages when the power produced by the PV panels is too high. In Chapter 3, we briefly describe the different classes of strategies that can be thought of for mitigating the voltage problems caused by PV panels. In Chapter 4, we propose and test a centralized active network management scheme for modulating the power injected by the inverters into the low-voltage network so as to avoid overvoltages. The chapter ends with a discussion about the fairness of the solution outputted by this centralized scheme. Chapter 5 presents our two distributed control schemes. One modulates only the active power delivered by the inverters while the other modulates both the active and reactive power. This chapter compares also the performances of these distributed schemes with those of the centralized one. Finally, Chapter 6 concludes this manuscript and discusses future work.

Chapter 2

Modeling of the system

In this chapter, we describe the model of the low-voltage network that will be used in our studies. The chapter starts with a general description of a low-voltage distribution network and a description of the modeling assumptions made for building our low-voltage test networks. This part is followed by a brief section that details the power flow equations linking the power injected into the test network to the voltages and currents. The chapter ends with simulation results showing that when the power injected by the panels into the test networks is not curtailed, these test networks may be prone to serious voltage issues.

2.1 Modeling assumptions

The low-voltage grids refer to the parts of the power grid whose nominal voltage is the lowest. This lowest voltage can vary from country to country. For example, it is equal to 230 V in Belgium and to 110 V in the US. One or several transformers connect the low-voltage grid to the medium voltage grid. In the power system jargon, these transformers are called MV/LV transformers where MV stands for Medium Voltage and LV for Low Voltage. Low-voltage grids are often referred to as feeders leaving MV/LV transformers. As mentioned already several times earlier, our goal is to design strategies to control the active and reactive power injected by the PV panels into the distribution grid so as to ensure that the voltages stay within their limits. As a consequence, our research requires models that are able to catch the relation between these power injections and the voltages of the network. For the

electrical parts of the network, different levels of modeling are possible. Given the span of this master thesis, we only consider the low voltage part of the distribution network, namely a feeder starting from the MV/LV transformer. Moreover, we will adopt for transformers and lines of the low-voltage grid a level of modeling usually considered in transmission network for studying voltage problems. This level of modeling assumes that the three-phases are balanced. As a result, only one line is required for modeling the different phases. Note that this assumption should probably be revised in future work. Indeed, low-voltage distribution networks are known for not being well-balanced, since residential loads are usually single phase. Houses are often also only connected to a single phase, as mentioned in the Electric Power Distribution Handbook [16]. Furthermore, PV panels under 5 kVA are often also only connected to a single phase [9]. Figure 2.1 gives a simple representation of the network studied in this master thesis. Note that we will assume throughout this manuscript that the thermal limit of this network can never be reached.

In the subsequent subsection, we detail all the other modeling assumptions.

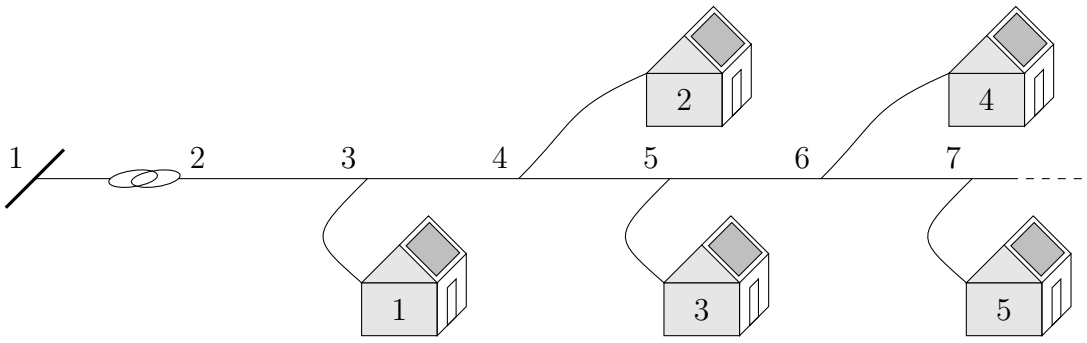

Figure 2.1: Graphic representation of the test network.

2.1.1 Equivalent for the higher voltage system

The voltages and the currents in the low-voltage grid obviously depend on the characteristics of the power system as seen from the MV/LV junction. We model the power system that comes atop of the MV/LV transformer and the transformer itself by a Thévenin equivalent, that is, our test network is connected to an infinite bus — whose voltage is the one from the Thévenin equivalent V_1 — trough an impedance Z_{12}. An infinite bus is a node whose voltage magnitude stays constant. Additionally, this voltage is assumed to always oscillate at the nominal frequency. When doing

load-flow computations (see Section 2.3), this node will serve as slack bus. Note that with such a modeling choice, we implicitly assume that the control strategies implemented at the low-voltage level do not modify the voltages in other parts of the network. The assumption is arguable in many situations, such as for example those for which the electrical distances between the low-voltage network and the generators of the system are high.

2.1.2 Houses

A house is referred by its number j. The symbol $nbHouse$ gives the number of houses connected to the low-voltage network. A house is made of two parts: a PV installation and domestic loads. Models for these two parts are proposed in subsections 2.1.4 and 2.1.5.

2.1.3 Nodes and lines

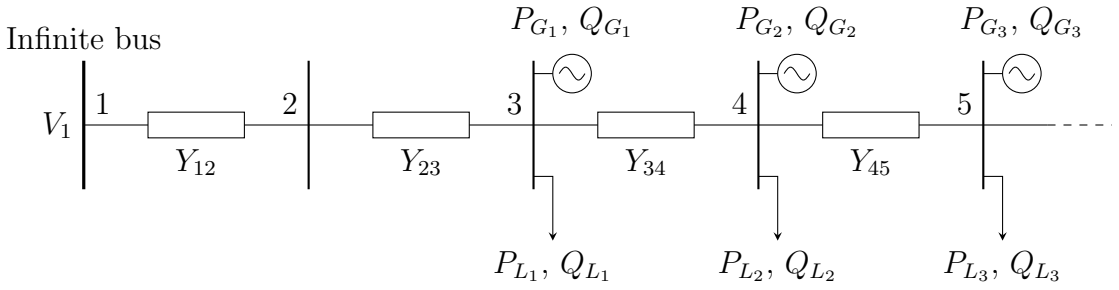

Figure 2.2: Electrical model of the network.

A node is a point of the low-voltage grid to which an element (house, transformer, etc.) is connected. In this manuscript, nodes are referred to by numbers. The node 1 is the node the infinite bus system is connected to. The node 2 is the node that connects the Thévenin equivalent of the external grid to the low-voltage grid. The node n ($n > 2$) is the node that connects the house $n - 2$ to the low-voltage grid. We use the symbol N to define the number of nodes in our low-voltage network. We have that the number of nodes is equal to the number of houses plus two.

A line refers here to the piece of the electrical network that connects two nodes. The line ij is the line that connects node i to node j. The electrical characteristics of

line ij are defined by its reactance X_{ij} and its resistance R_{ij}. These two elements define the electrical impedance Z_{ij} of the line in the following way: $Z_{ij} = R_{ij} + jX_{ij}$. The electrical impedance is the measure of the opposition that a circuit presents to the passage of a current when a voltage is applied. Typical values for the resistance and the reactance of a line of a low-voltage grid are expressed in Ohm/km. Both resistance and reactance have the same order of magnitude of a few tenth of Ohm per kilometer [2]. In the case of underground cables, the reactance value is lower. The admittance is defined as the inverse of the impedance. We use the symbol Y_{ij} to denote the admittance of line ij.

Figure 2.2 is the one-line diagram of the test network. The interconnection of all electrical elements can be found in this diagram.

Let us define the admittance matrix of our low-voltage distribution network as follows:

$$\mathbf{Y} = \begin{pmatrix} Y_{12} & -Y_{12} & 0 & 0 & \cdots & 0 \\ -Y_{12} & Y_{12}+Y_{23} & -Y_{23} & 0 & \cdots & 0 \\ 0 & -Y_{23} & Y_{23}+Y_{34} & -Y_{34} & \cdots & 0 \\ 0 & 0 & -Y_{34} & Y_{34}+Y_{45} & \cdots & 0 \\ \vdots & \vdots & \vdots & \vdots & \ddots & -Y_{(N-1,N)} \\ 0 & 0 & 0 & 0 & -Y_{(N-1,N)} & Y_{(N-1,N)} \end{pmatrix} . \quad (2.1)$$

This admittance matrix catches all the electrical characteristics of our low-voltage network.

Let $\overline{I}_i$ be the phasor of current injected at bus i, $\overline{V}_i = |V_i|e^{j\theta_i}$, the phasor of voltage at bus i and $\mathbf{Y}_{ik} = G_{ik} + jB_{ik} = |Y_{ik}|e^{j\gamma_{ik}}$, the element (i,k) of the admittance matrix $\mathbf{Y}$, it can be shown that

$$\overline{I} = \mathbf{Y}\overline{V} = \sum_{k=1}^{N} \mathbf{Y}_{ik}\overline{V}_k \ . \quad (2.2)$$

In Section 2.3, we will use this admittance matrix to compute the currents and the voltages in the system from the active and the reactive power injected at the different nodes.

2.1.4 PV installations

A PV installation is made of two key elements: PV panels that generate DC current and a power converter that transforms this DC current into an AC one, namely an inverter. The PV installations are modeled by two single values: the active and the reactive power that they inject into the network. For the PV installation of house j, these two values will be referred to by P_{G_j} and Q_{G_j}, respectively. Note that we assume here that the electrical impedance of the cable connecting the power converter to the feeder of the low-voltage network is equal to zero.

We will also assume that these values are controllable, provided that they stay within their physical limits. These limits are assumed to be the following ones:

1. The active power injected into the network needs to be greater than 0, i.e. $P_{G_j} > 0 \quad \forall j$.
2. The active power injected into the network needs to be smaller than the maximum amount of power that can be generated by the PV installation. Let $P_{G_j}^{\max}$ denote this maximum amount of power. Note that in this work $P_{G_j}^{\max}$ is assumed to depend only on sunshine. This may be a quite limitative assumption since once it starts delivering active power, a PV installation may take a few instants to reach its maximum power output.
3. Since the current outputted by the PV inverter is limited for technical reasons, we consider a limit on the apparent power delivered by the PV installation j. It has to stay below $S_j^{\max}$. The apparent power S_j outputted by installation j can be computed from active and reactive powerin the following way:

$$S_j = \sqrt{P_{G_j}^2 + Q_{G_j}^2} \, . \tag{2.3}$$

2.1.5 Loads

The loads of a house j are modeled by an equivalent PQ load. The symbol P_{L_j} (resp. Q_{L_j}) will refer to the active (resp. reactive) power of the equivalent load for house j. Note that we do not model here the relation that exists between the load consumption and the voltage, which is quite arguable, especially since we are studying voltage problems.

2.2 Network data

In our simulations, different test networks of the type of the generic one presented in Section 2.1 will be used. For every of these test networks, we assume that

1. the electrical distances between two neighboring houses are the same and all electrical cables have the same electric properties, i.e. $Y_{i,i+1} = Y_{j,j+1}\ \forall i, j \in \{2, 3, \ldots, nbHouse + 1\}$,
2. $P_{G_i}^{\max} = P_{G_j}^{\max}\ \forall i, j \in \{1, 2, \ldots, nbHouse\}$,
3. $P_{L_i} = P_{L_j}\ \forall i, j \in \{1, 2, \ldots, nbHouse\}$,
4. $Q_{L_i} = 0\ \forall i \in \{1, 2, \ldots, nbHouse\}$,
5. the nominal voltage of the network is 400 V,
6. the value of the impedance of the Thévenin equivalent Y_{12} is equal to $0.0059 + j0.0094\ \Omega$,
7. the value of Thévenin voltage is equal to 420 V.

As a consequence, for having a fully defined test network, we just need to define the four following quantities: the number of houses, the impedance between two neighboring houses, the maximum power production of a PV installation and the active power consumption of a load. Note that when defining test networks, we will not give directly the value of the impedance between two neighboring houses but well the length of the line connecting two neighboring houses and the resistance and reactance of the line expressed in Ω/km.

In all the computations done for this manuscript, we will not use the physical units for power, voltage, current, impedance and admittance. Instead, we will use the per-unit system, which expresses the system quantities as fractions of a defined base unit quantity. In this per unit system, similar types of apparatus installed at different voltage levels will have impedances, voltage drops and losses that are similar, even if the unit size varies widely.

A per-unit system provides base units for power, voltage, current, impedance, and admittance. Only two of these units are independent. In this manuscript, we choose the base voltage V_{base} and the base power S_{base} as being the two independent units. More specifically, we set V_{base} equal to 400 V and S_{base} equal to 630 kVA, which is a typical nominal power for a MV/LV transformer. From these values, we compute

the base impedance:

$$Z_{base} = \frac{V_{base}^2}{S_{base}} = \frac{(400\text{ V})^2}{630\text{ kVA}} = 0.254\ \Omega\ , \tag{2.4}$$

the base admittance:

$$Y_{base} = \frac{1}{Z_{base}} = 3.938\text{ S}\ , \tag{2.5}$$

and the base current:

$$I_{base} = \frac{S_{base}}{\sqrt{3}V_{base}} = \frac{630\text{ kVA}}{\sqrt{3}\cdot 400\text{ V}} = 909\text{ A}\ . \tag{2.6}$$

For the sake of additional clarity, we write hereafter the expressions used for transforming the physical units for power, voltage, current, impedance and admittance into a per-unit system.

$$V_{p.u.} = \frac{V_{volt}}{V_{base}} \quad P_{p.u.} = \frac{P_{watt}}{S_{base}} \quad Z_{p.u.} = \frac{Z_{ohm}}{Z_{base}} \quad I_{p.u.} = \frac{I_{ampere}}{I_{base}} \quad Y_{p.u.} = \frac{Y_{siemens}}{Y_{base}} \tag{2.7}$$

Table 2.1 gathers the numerical values of the first test network used in our simulations. These typical values were drawn from reference [2]. Those values were also used in [4].

Table 2.1: Model data.

Nominal voltage	400 V
Line resistance	0.24 Ω/km
Line reactance	0.1 Ω/km
Number of houses	18
Distance between houses	50 m
Active power production of PV panels (P_{G_j})	0 kW
Reactive power production of PV panels (Q_{G_j})	0 kvar
House active power consumption (P_{L_j})	10 kW
House reactive power consumption (Q_{L_j})	0 kvar

We note that when presenting the simulation results, the voltages will always be expressed in the per-unit system. However, results involving power will always be converted back to physical units.

2.3 Power flow

In order to be able to assess the impact of PV generation on our test networks, we need a tool that can compute, from the power injected into the grid by the PV panels and the power drawn by the loads from the grid, the currents in the lines and the voltages at the buses. This tool is referred to, in the power system community, as a load-flow. It is certainly the most well-known and used computational tool in power systems. The main idea behind this tool is first to express the net power injected into the network as a function of the voltage magnitudes and angles. Afterwards, these so-called *load-flow equations* are solved to compute the voltages. From these quantities, the currents can be computed in a straightforward way using the equation $\overline{I} = Y\overline{V}$.

We now explain how to derive the load-flow equations. Let $\overline{I}_i$ and $\overline{V}_i$ be the complex current injected at node i and the complex voltage at node i, respectively. Let S_i be the complex power injected into the network at node i. By definition, $S_i = P_i + jQ_i$ where P_i (Q_i) is the net active (reactive) power injected into the network at node i. Note that the net active (reactive) power P_i (Q_i) is the difference between the active (reactive) power injected by a generation source at this node and the active (reactive) power drawn from the load connected at this node. We can also write:

$$\begin{aligned} S_i &= \overline{V}_i \cdot \overline{I}_i^* && (2.8)\\ &= \overline{V}_i \cdot \sum_{k=1}^{N} \mathbf{Y}_{ik}^* \overline{V}_k^* && (2.9)\\ &= \sum_{k=1}^{N} \mathbf{Y}_{ik}^* \overline{V}_i \overline{V}_k^* && (2.10)\\ &= \sum_{k=1}^{N} |Y_{ik}||V_i||V_k| e^{j(\theta_i - \theta_k - \gamma_{ik})} \ . && (2.11) \end{aligned}$$

By taking the real part and the imaginary part of (2.11), we obtain the two characteristic equations of a load-flow problem ((2.12) and (2.13)).

$$P_i = \sum_{k=1}^{N} |Y_{ik}||V_i||V_k| \cos(\theta_i - \theta_k - \gamma_{ik}) \qquad i = 2, 3, \ldots, N \qquad (2.12)$$

$$Q_i = \sum_{k=1}^{N} |Y_{ik}||V_i||V_k| \sin(\theta_i - \theta_k - \gamma_{ik}) \qquad i = 2, 3, \ldots, N \tag{2.13}$$

As mentioned above, houses are connected from bus 3 to the last bus. Bus 1 is the slack bus and there is no power injected or consumed at bus 2 (P_2 and Q_2 are equal to zero). Power flow equations can be divided in two subsets: equations related to buses with no house connected ((2.14) and (2.15)) and equations related to buses connected to a house ((2.16) and (2.17)).

$$0 = \sum_{k=1}^{N} |Y_{(2,k)}||V_2||V_k| \cos(\theta_2 - \theta_k - \gamma_{(2,k)}) \tag{2.14}$$

$$0 = \sum_{k=1}^{N} |Y_{(2,k)}||V_2||V_k| \sin(\theta_2 - \theta_k - \gamma_{(2,k)}) \tag{2.15}$$

$$P_{j+2} = P_{G_j} - P_{L_j} = \sum_{k=1}^{N} |Y_{(j+2,k)}||V_{j+2}||V_k| \cos(\theta_{j+2} - \theta_k - \gamma_{(j+2,k)}), \tag{2.16}$$
$$j = 1, 2, \ldots, nbHouse$$

$$Q_{j+2} = Q_{G_j} - Q_{L_j} = \sum_{k=1}^{N} |Y_{(j+2,k)}||V_{j+2}||V_k| \sin(\theta_{j+2} - \theta_k - \gamma_{(j+2,k)}), \tag{2.17}$$
$$j = 1, 2, \ldots, nbHouse$$

Furthermore, given that the network is made of a single line, the $\mathbf{Y}$ matrix has a special form. It is a tridiagonal matrix, i.e. $\mathbf{Y}_{ij} = 0$ if $j \neq i-1, i$ or $i+1$. In the particular context of our generic test problem, the sum in (2.14) to (2.17) can thus be simplified.

$$0 = \sum_{k=1}^{3} |Y_{(2,k)}||V_2||V_k| \cos(\theta_2 - \theta_k - \gamma_{(2,k)}) \tag{2.18}$$

$$0 = \sum_{k=1}^{3} |Y_{(2,k)}||V_2||V_k| \sin(\theta_2 - \theta_k - \gamma_{(2,k)}) \tag{2.19}$$

$$P_{G_j} - P_{L_j} = \sum_{k=j+1}^{j+3} |Y_{(j+2,k)}||V_{j+2}||V_k| \cos(\theta_{j+2} - \theta_k - \gamma_{(j+2,k)}), \tag{2.20}$$
$$j = 1, 2, \ldots, nbHouse - 1$$

$$Q_{G_j} - Q_{L_j} = \sum_{k=j+1}^{j+3} |Y_{(j+2,k)}||V_{j+2}||V_k| \sin(\theta_{j+2} - \theta_k - \gamma_{(j+2,k)}), \tag{2.21}$$
$$j = 1, 2, \ldots, nbHouse - 1$$

$$P_{G_j} - P_{L_j} = \sum_{k=j+1}^{j+2} |Y_{(j+2,k)}||V_{j+2}||V_k| \cos(\theta_{j+2} - \theta_k - \gamma_{(j+2,k)}) \quad j = nbHouse \tag{2.22}$$

$$Q_{G_j} - Q_{L_j} = \sum_{k=j+1}^{j+2} |Y_{(j+2,k)}||V_{j+2}||V_k| \sin(\theta_{j+2} - \theta_k - \gamma_{(j+2,k)}) \quad j = nbHouse \tag{2.23}$$

Equations (2.18) to (2.23) form a system of $2N - 2$ non-linear equations. There are two equations for each bus, minus the infinite bus (slack bus) because voltage and angle are set as a reference at this one. Active and reactive power injected at each bus is known : P_i and Q_i for $i = 2, 3, \ldots, N$. The unknowns are the voltage amplitude and angle at each nodes, i.e. V_i and θ_i for $i = 2, 3, \ldots, N$. The system can be solved numerically using for example Newton-Raphson method. In MATLAB, we used the function *fsolve* to solve the system of non-linear equations.

For readers interested to know more about load-flows, we advise them to consult standard textbooks in power systems, such as for example [8], [11] and [17].

2.4 Simulation results

The section reports and discusses results obtained when running load-flow analyses on our test network. The first test network on which we run a load-flow analysis is a network for which the PV installations do not inject any power into the system. The data of this network are given in Table 2.1. The second test network differs only from the first one by the fact that the power injected by the PV panels into the network is equal to 7 kW and that house consumption is set to 1 kW. The data of this network are given in Table 2.2.

Table 2.2: Second test network data.

Nominal voltage	400 V
Line resistance	0.24 Ω/km
Line reactance	0.1 Ω/km
Number of houses	18
Distance between houses	50 m
Active power production of PV panels (P_{G_j})	7 kW
Reactive power production of PV panels (Q_{G_j})	0 kvar
House active power consumption (P_{L_j})	1 kW
House reactive power consumption (Q_{L_j})	0 kvar

2.4.1 First test network: no PV generation

Figure 2.3 reports the voltages at the different nodes of our test system where there is no PV generation.

The blue crosses show voltage magnitudes and the green bullets voltage angles. As we can see, the voltage is maximal for node 1 to which the infinite bus system is connected. Naturally, it is equal to 1.05 p.u. The further we go into the feeder, the more the voltage magnitude decreases. At the last node of the system, it is slightly above 0.9 p.u.

By increasing the load consumption, even lower voltages at this node could be observed. Note that distribution networks with no distributed generation sources were planned so as to avoid overvoltages at the beginning of the LV line during light

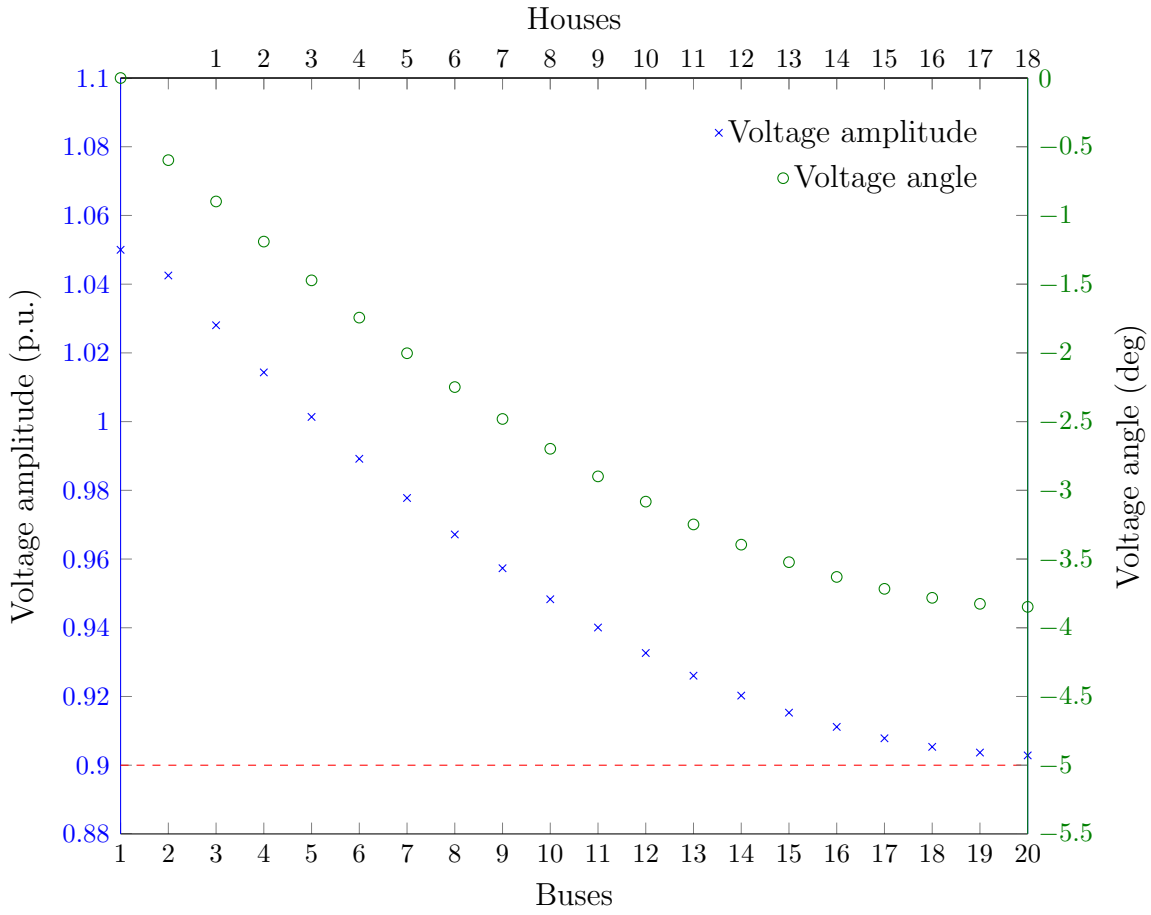

Figure 2.3: Voltage profile of the street without PV generation.

loading period and undervoltages at the end of the line during heavy loading. The green bullets give the voltage angles at the different nodes. As we can see, the angles decrease when going into the direction of the end of the feeder. Note that with a larger line reactance, larger decreases would be observed.

2.4.2 Second test network: PV generation equal to 7 kW per house

Figure 2.4 shows the voltages at the different nodes of the street for our second test network. As can be seen, the further we go into the street, the larger the voltages

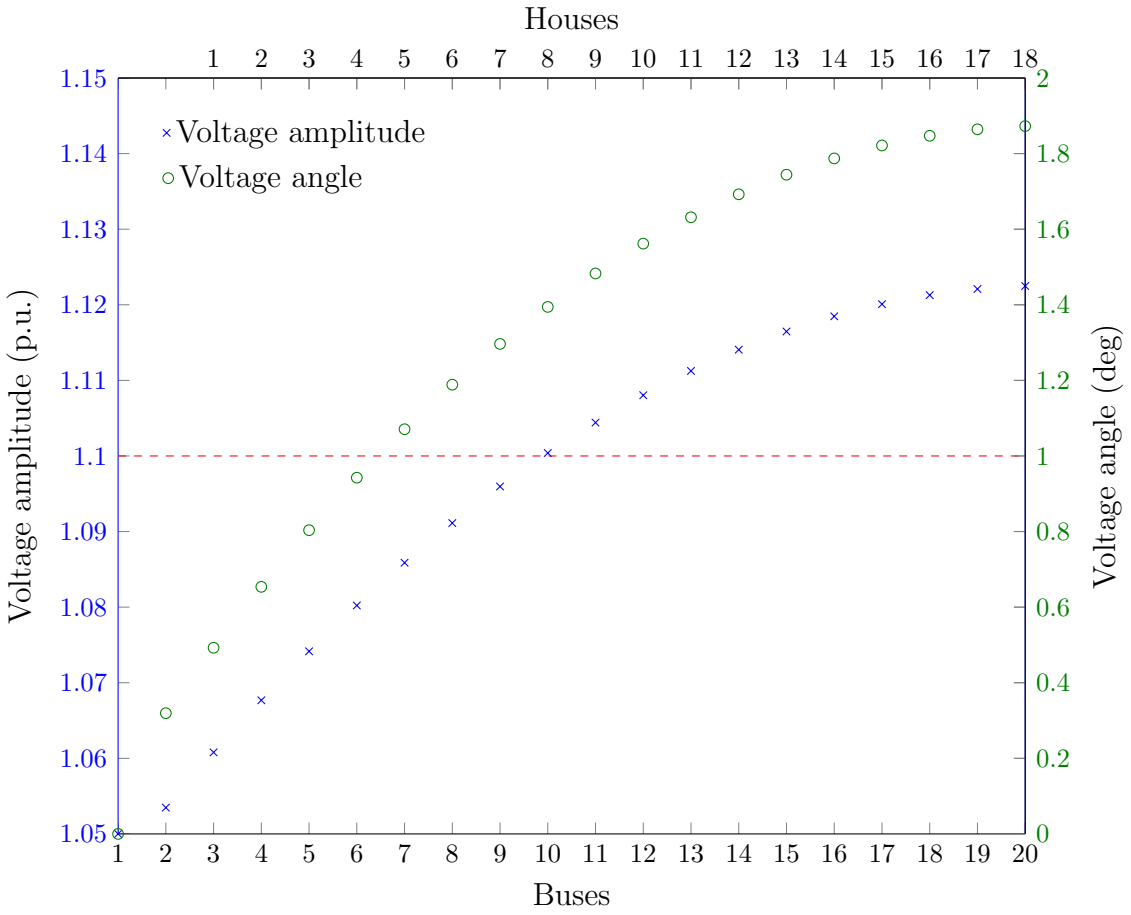

Figure 2.4: Voltage profile of the street with PV generation.

are. This behavior is explained by the fact that the PV installation of every house produces an amount of power (7 kW) larger than its load consumption (1 kW). As a result, there is a power flow reversal that leads to this increase in voltages. Note that the voltage reaches at the end of the line a value slightly above 1.12 p.u., which is problematic. Indeed, in low-voltage network, the largest voltage deviation around the nominal value should be limited to 0.1 p.u.

In Chapter 3, we will discuss different types of strategies that could be implemented for avoiding such overvoltage problems to happen.

Chapter 3

Generic strategies for avoiding voltage problems

We briefly describe in this chapter the different classes of strategies that we can envision for avoiding voltage problems. These strategies can be classified into two major categories: fit and forget *and* Active Network Management (ANM). *We report also simulation results highlighting the effect of such strategies on the test system presented in the previous chapter.*

3.1 Introduction

We have seen previously that PV panels connected to the low-voltage network can cause unacceptable voltage rises. Two main different classes of strategies could be thought of for avoiding those problems. For the first class, the DSO would seek to enforce its *fit and forget* doctrine by either investing in new lines in its distribution network or by simply denying the connection of new PV installations to its network. In Section 3.2, we will illustrate on our test network the effect of different new investments on the voltages.

Unfortunately, building new lines has a cost and refusing to new sources of renewable energy the access to the network may be unpopular (especially if people are heavily subsidized for installing PV panels, as it was the case until very recently in Wallonia)

and against European directives.[1] This is why DSOs are heavily pushed to rather develop another class of strategies known as *active network management*. Active network management schemes actively control the load, the transformers settings, the power injected by renewables into the distribution grid, etc. in order to avoid network problems. We illustrate the potential effect of such strategies on our test system in Section 3.3.

In the next chapter, we will discuss a centralized active network management scheme for modulating, in an optimal way and in real-time, the active and reactive power injected by the PV panels into the low-voltage network, so as to avoid voltage problems.

3.2 Fit and forget

We now come back to our problematic test system of Chapter 2 and show that new investments in the low-voltage grid could indeed solve these overvoltage problems.

First, we suppose that the DSO has decided to replace the low-voltage feeder by one whose impedance is twice less that the one of the original feeder. Note that a feeder with a lower impedance has a larger section and would therefore be more expensive. As we can see on Figure 3.1, the new feeder mitigates the voltage rise due to PV panels. Note that since the MV/LV transformer and the network coming ahead of it are modeled as a Thévenin equivalent, it would still be possible to observe, for this test system, unacceptable voltage rises with an increase of the power injected by the PV panels into the network, whatever the impedance of the feeder.

Rather than building a new feeder, the DSO could also for example connect directly the last house of our test system to the MV/LV transformer by building a new line, as shown on Figure 3.2. The plots of Figure 3.3 shows (i) the new voltages observed when the impedance of this line is equal to the impedance between the transformer and the last house of the original test system, (ii) the voltages obtained when the impedance of this new line is twice less, and (iii) the voltages when this impedance is equal to the one between two houses. We observe that:

[1] Cf. Directive 2009/28/EC of the European Parliament and of the Council of 23 April 2009 on the promotion of the use of energy from renewable sources and amending and subsequently repealing Directives 2001/77/EC and 2003/30/EC, Article 16, paragraph 2 and following (see [1]).

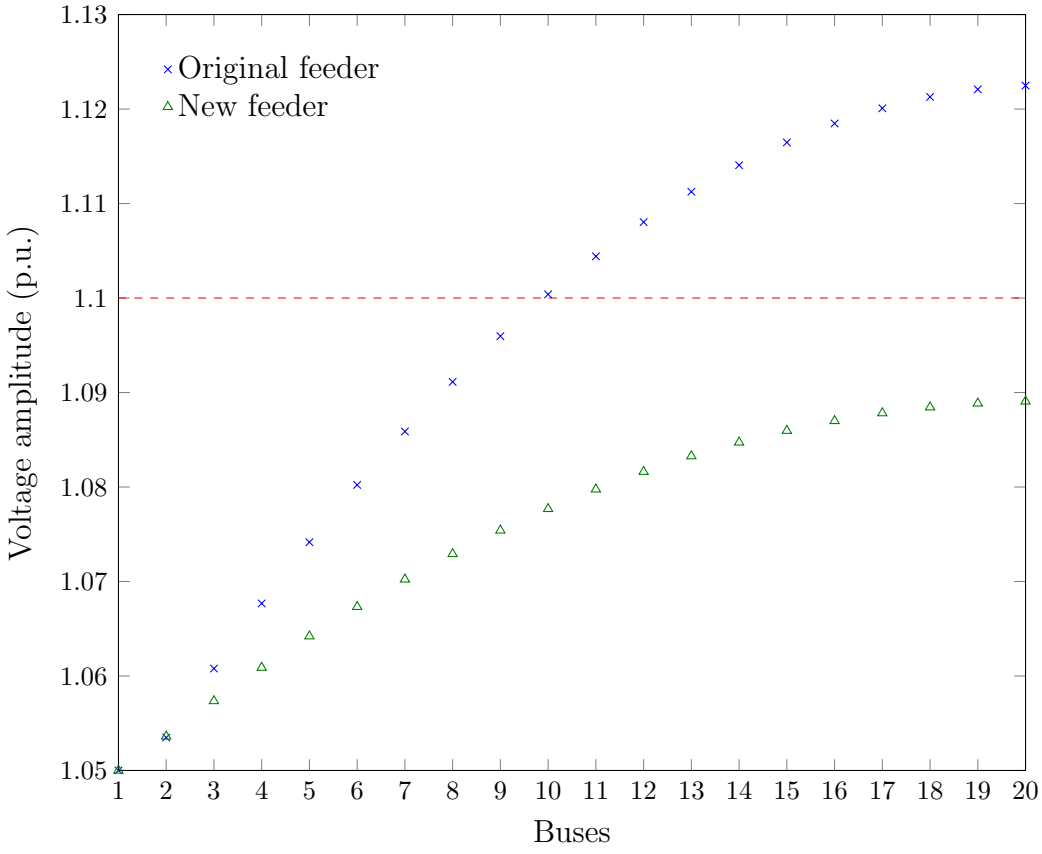

Figure 3.1: Voltage profile for a feeder with an impedance twice less than the one of the original feeder (resistance of 0.12 Ω/km and reactance of 0.05 Ω/km).

- these new lines cause a voltage drop;
- the voltage drop is more important when the impedance of this new line is smaller.

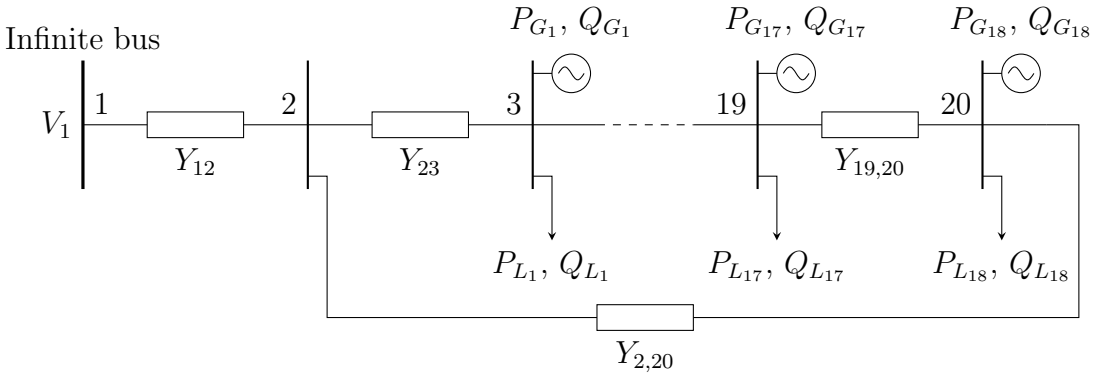

Figure 3.2: Electrical model of the test network when a new line is added from bus 20 to bus 2.

Similarly to capacitor banks that are used to rise voltages in case of undervoltages, another solution could be to install at the end of the street a inductor bank that would automatically be switched on when the voltage at the end of the street becomes too high. As can be seen in Figure 3.4, when a load of 50 kvar is added at bus 20, voltages are significantly lower than in the original case.

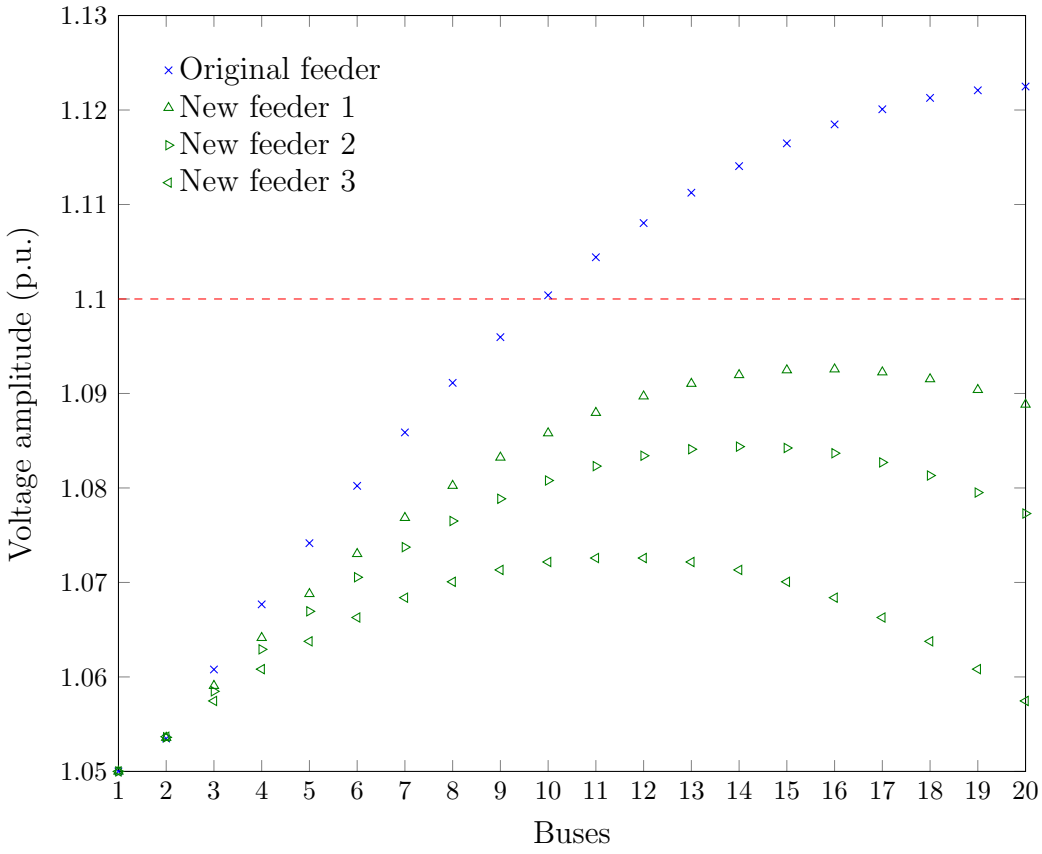

Figure 3.3: Voltage profile of the feeder when a line is added to connect the last house of the street to the MV/LV transformer. Let Y_{line} be the admittance between two houses. In the case of feeder 1, the admittance of the new line is equal to $Y_{line}/18$, that is, the same admittance as the line of the whole street. For feeder 2, it is equal to half this value, i.e. $Y_{line}/9$ and for feeder 3, it is equal to the admittance between two houses, i.e. Y_{line}.

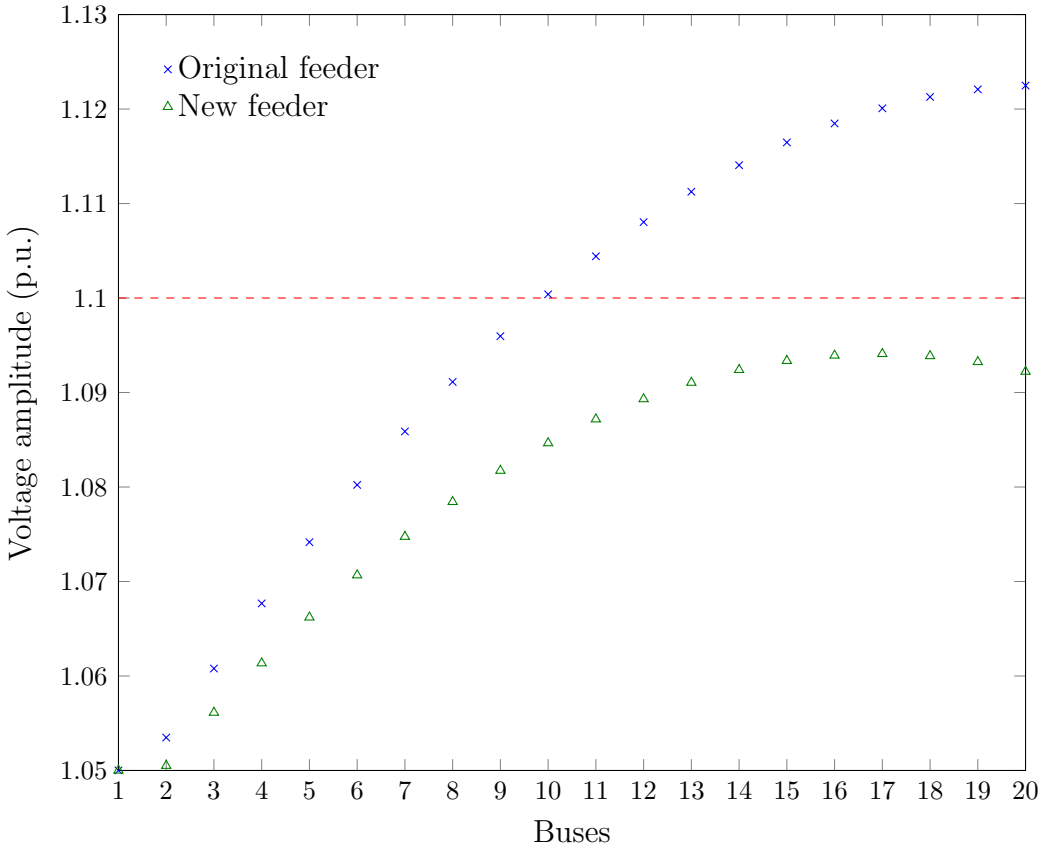

Figure 3.4: Voltage profile of the network when a purely reactive load of 50 kvar is added at bus 20.

3.3 Active network management

In the context of our test network, active network management schemes would dynamically modify one or several of the following variables: P_{L_j}s, Q_{L_j}s, P_{G_j}s and Q_{G_j}s, so as to avoid voltage problems. We may also think that it would be possible for the DSO to use control variables coming ahead of the low-voltage feeder. Those could be for example the ratio of transformers or the reactive power injected by wind farms at the medium-voltage level. They could indeed lower the voltage in the problematic low-voltage feeders.

In this manuscript, we will focus on the development of active network management schemes based only on the control of the active and reactive power injected (the P_{G_j}s and Q_{G_j}s) by the inverters into the network. While we have already seen in this manuscript that modifying the P_{G_j} could influence the voltages, we end this chapter by discussing an experiment that studies the influence of the Q_{G_j}s on the voltages. This experiment has been carried out by running a load-flow on our problematic test system where the Q_{G_j} has been chosen equal to $-\frac{1}{2}P_{G_j}$, that is, where the inverters draw from the network an amount of reactive power equal to half the amount of active power they inject into it. Figure 3.5 shows the voltages obtained. We can see that by drawing reactive power from the network, the voltages decrease. Notice that some of them are still higher than 1.1 p.u. In practice, the amount of reactive power an inverter can inject into the network or draw from the network is limited by the two following constraints: (i) the apparent power $S_j = \sqrt{P_{G_j} + Q_{G_j}}$ is constrained to stay below a limit value, (ii) the power factor $\cos\varphi$ of the installation should be limited to the interval $[(\cos\varphi)_{\min}, (\cos\varphi)_{\max}]$. In the case of DC load, the power absorbed is equal to the DC current of the load multiplied by the DC voltage. When it comes to AC load, the power absorbed is the product of the RMS value of the current, the RMS value of the voltage and the power factor, which is equal to the cosine of the phase shift between the voltage and the current. This power factor defines the active power consumed by the load. At its maximum 1, the load only absorbs active power and at its minimum, the load absorbs or produces only reactive power. Current inverters can produce or absorb power with a power factor ranging from 0.8 to 1.

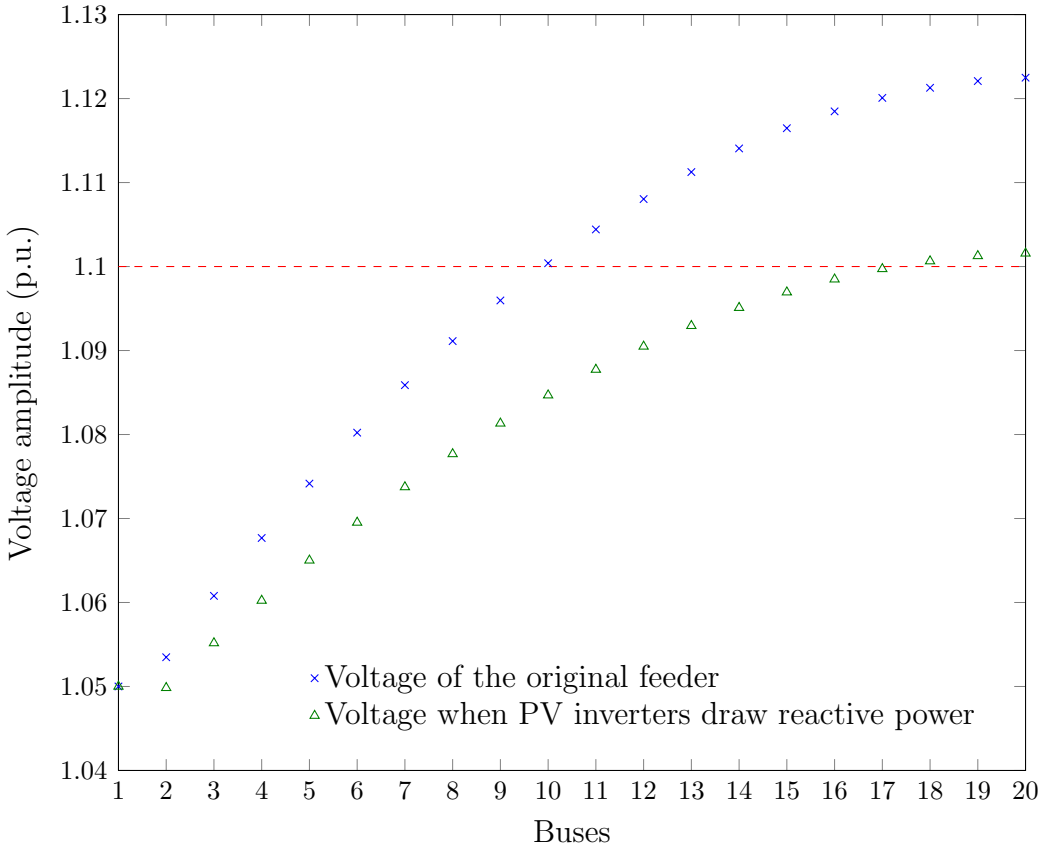

Figure 3.5: Voltage profile of the network when $Q_{G_j} = -\frac{1}{2}P_{G_j}$, with unchanged values of P_{G_j}s (7000 W).

Chapter 4

Centralized solution

In this chapter, we detail a centralized active network management scheme for modulating the active and reactive power of the inverters so as to avoid voltage problems. The chapter starts by discussing the technical challenges for implementing such a centralized scheme. Afterwards, a first logic for computing the orders to be sent from the centralized controller to the inverters is proposed. This logic aims at minimizing the amount of power curtailed. This part is followed by a discussion related to the poor fairness of the solution obtained. The chapter ends by proposing strategies for addressing this fairness issue.

4.1 Introduction

In the previous chapter, we have listed a few strategies for solving the voltage problems arising when the PV installations inject too much power into the low-voltage network. Among those strategies, we proposed one that was based on the modulation of the active and reactive power injected by the inverters into the grid. In this chapter, we are going to further study this strategy in a context where we assume that the modulation orders are computed by a centralized entity that communicates with the PV installations and the loads.

In the next section (Section 4.2), we will discuss the technical infrastructure that needs to be put in place for implementing such a scheme. Afterwards, in Section 4.3, we will propose a first logic to be used by the centralized controller for computing the modulation orders. It is based on the resolution of an optimization problem

whose cost function is the amount of power curtailed. In the same section, we will also discuss the simulation results obtained on our test system. The section that follows will start by an analysis of the fairness of the solution computed by the centralized controller. By anticipating the result of this analysis, we will observe that its solution is not fair in the sense that the PV installations at the end of the street are significantly more curtailed than those installed at the beginning. As a result, owners of those installations bear a higher financial prejudice. To overcome this problem of fairness, we will propose two types of strategies. One is based on the introduction of a financial compensation mechanism. The other is based on a reformulation of the optimization problem so as to have fairer modulation orders.

4.2 Technical challenges for building the centralized scheme

A centralized control scheme is made of three different parts. The first part is all the elements on which it relies for acquiring information about the system it controls. The second part is the "brain" of the scheme, something that is usually called the controller in the control literature. It computes, from the (history of) information, control actions. The third and last part is the infrastructure used for sending and applying its control actions. We discuss in the next subsections the main elements of infrastructure that needs to be put in place to build a centralized control scheme for our test system.

4.2.1 First part: information gathering

This part is typically composed of sensors used for measuring physical values and of a communication infrastructure for sending them to the "brain" of the "control scheme".

In the next section, we will see that for computing the modulation orders, our scheme needs, in the context of the test system presented in Chapter 2, a full knowledge of the system. The only elements describing this system that can change over time are the following: the (active and reactive) power of the loads (P_{L_j} and Q_{L_j} $\forall j \in \{1, 2, \ldots, nbHouse\}$) and the maximum amount of power that the PV installations can generate ($P_{G_j}^{\max}$). Therefore, only the values of the P_{L_j}s, the Q_{L_j}s and $P_{G_j}^{\max}$s need to be measured at a *sufficient rate* and sent to the "brain" of the

scheme. Note that the P_{G_j}s and the Q_{G_j}s can also change with time but these values do not need to be measured and sent to the "brain" since they are the values of the control actions. Therefore, the infrastructure needs to have (i) sensors able to measure all the P_{L_j}s, Q_{L_j}s and $P_{G_j}^{max}$s (ii) communication channels able to transfer these measurements from the houses to the centralized controller. As communication channels, different technologies exist. For example, internet connections or General Packet Radio Service (GPRS) connections can be used. We could also think about using Power Line Communication (PLC) that carries data on the AC line. Mix of several communication technologies could also be used. For example, the data of the houses could be transmitted using a PLC-based technology to the nearest substation from which GPRS technology would be used for transferring them to the centralized controller.

In the previous paragraph, we mentioned that these measurements need to be sent at a sufficient rate to the centralized controller. We may wonder what is meant by "sufficient rate". Loosely speaking, we may say that this rate is sufficient if by increasing it, the performance of the control scheme cannot increase significantly anymore.

In the sequel of this document, we will assume (i) that all the measurements are synchronized and (ii) that the time between two different sets of measurements is equal to Δt seconds. We will also use discrete time indexes $0, 1, \ldots, t, t+1, \ldots$ to specify to which time instant a variable is referring to. For example, $P_{L_j,t}$ will refer to the value of the active power of the load connected to node $j+2$ at discrete time instant t and $P_{L_j,t+1}$ to its value Δt seconds later.

4.2.2 Second part: the "brain" for storing and processing the information

The second part of the infrastructure is related to the machinery needed for storing the information gathered about the system and processing this information. As we will see later, our logic for computing the control actions exploits only the last set of measurements. The requirements for memory are therefore very low. As for the computational requirements, they need to be sufficient to be able to process rapidly enough the information for computing the control actions. In the next section, we will see that this processing of the information implies solving at every discrete time instant t an optimization problem having a number of variables equal to twice the number of houses. For our test system, this problem can be solved in a matter of a

few hundreds of milliseconds on a standard computer.

4.2.3 Third part: from computational results till applied actions

Once the actions have been computed by the centralized controller, they need to be applied on the system.

For our test system, this implies to have a communication channel between the "brain" of the centralized controller and the inverters. This also implies having inverters which are able to modify upon request the amount of active and reactive power they inject into the system.

4.3 The centralized logic

In this section, we explain the centralized logic used by the controller for computing the modulation orders. This section is structured as follows. First, in Subsection 4.3.1, we show in the particular case where the P_{L_j}s, Q_{L_j}s and $P_{G_j}^{\max}$s are assumed to be constant, how the logic behind our control scheme computes the values P_{G_j}s and Q_{G_j}s to be sent to the inverters. Subsection 4.3.2 discusses the more realistic case where the P_{L_j}s, Q_{L_j}s and $P_{G_j}^{\max}$s are not constant. In Subsection 4.3.3, we discuss simulation results.

Before going further into this section, we stress that the logic of the centralized controller is specific to the test system presented in Chapter 2. However, it could be extended in a not so laborious way to more complex low-voltage distribution networks, such as meshed ones.

4.3.1 Optimization problem for computing the modulation orders

We are here in a context where the P_{L_j}s, Q_{L_j}s and $P_{G_j}^{\max}$s are constant. The controller knows these values, the $S_j^{\max}$s, the admittance matrix of the system and the Thévenin equivalent used for modeling the MV/LV transformer as well as the power system coming atop of this transformer. The controller can modulate the amount of active

power and reactive power injected by the inverters into the network or, equivalently, it can set the values of P_{G_j} and Q_{G_j} $\forall j \in \{1, 2, \ldots, nbHouse\}$. The controller has for objective to compute the modulation orders to be sent to the converters so as to avoid voltage problems that plague the network. But, the difficulty comes from the fact that it does not just have to compute a modulation order that avoids such problems. Indeed, it also wants its modulation orders to have a low cost. We define here the cost of modulation orders as being the difference between the maximum amount of power that the PV installations could inject into the network ($\sum_{j=1}^{nbHouse} P_{G_j}^{\max}$) and the amount of power the PV installations actually inject after application of the modulation orders ($\sum_{j=1}^{nbHouse} P_{G_j}$).

The problem of finding the right modulation orders can therefore be formalized as follows:

Program 1: OPF problem

Find the modulation orders $P_{G_1}, P_{G_2}, \ldots, P_{G_{nbHouse}}, Q_{G_1}, Q_{G_2}, \ldots, Q_{G_{nbHouse}}$ such that ($\sum_{k=1}^{nbHouse} P_{G_k}^{\max} - P_{G_k}$) is minimal and all the constraints are satisfied.

This type of optimization problem belongs the general class of "Optimal Power Flow" problems, vastly studied in the power system literature. Roughly speaking, this generic class of problem encompasses all the power system optimization problems where network constraints are taken into account. The reader who is interested to know more about Optimal Power Flow problems can refer to the following survey papers: [3],[6] and [10].

When solving OPF problems it is common to extend the set of optimization variables to the voltages and the angles at the different nodes of the system. By proceeding in this manner, the optimization problem can be written in a way such that it corresponds to the minimization of the cost function under a set of equality and inequality constraints where all the variables belong to the set of optimization variables. As a result, standard non-linear optimization techniques can be used for computing a solution.

A reformulation of our problem using this classical OPF trick leads to Program 2, where

- equation (4.1) defines the objective function;
- equation (4.2) is a generic way for writing the power flow equations (equations

(2.18) to (2.23) of Chapter 2);

- inequality (4.3) forces the voltages to stay within their limits;
- inequality (4.4) stresses that the active power injected by the inverters into the grid should always be positive and smaller than the maximal power that the PV panels can produce given current sunlight;
- inequality (4.5) has been introduced to model the reactive power compensation constraints, namely a limit on the power factor of the PV inverters and a limit on the apparent power that the inverters can deliver.

Program 2: Generic OPF

$$\min_{P_{G_j}, Q_{G_j}, |V_i|, \theta_i} \quad \sum_{k=1}^{nbHouse} P_{G_k}^{\max} - P_{G_k} \tag{4.1}$$

subject to

$$h(P_G, Q_G, |V|, \theta) = 0 \tag{4.2}$$

$$V^{\min} \leq |V_i| \leq V^{\max}, \qquad i = 2, 3, \ldots, N \tag{4.3}$$

$$0 \leq P_{G_j} \leq P_{G_j}^{\max}, \qquad j = 1, 2, \ldots, nbHouse \tag{4.4}$$

$$g^{\min} \leq g(P_{G_j}, Q_{G_j}) \leq g^{\max}, \qquad j = 1, 2, \ldots, nbHouse \tag{4.5}$$

By further specifying equation (4.2) and inequality (4.5), we obtain the rather long Program 3.

Program 3: Detailed OPF

$$\min_{P_{G_j},Q_{G_j},|V_i|,\theta_i} \quad \sum_{k=1}^{nbHouse} P_{G_k}^{\max} - P_{G_k} \tag{4.6}$$

subject to

$$0 = \sum_{k=1}^{3} |Y_{(2,k)}||V_2||V_k| \cos(\theta_2 - \theta_k - \gamma_{(2,k)}) \tag{4.7}$$

$$0 = \sum_{k=1}^{3} |Y_{(2,k)}||V_2||V_k| \sin(\theta_2 - \theta_k - \gamma_{(2,k)}) \tag{4.8}$$

$$P_{G_j} - P_{L_j} = \sum_{k=j+1}^{j+3} |Y_{(j+2,k)}||V_{j+2}||V_k| \cos(\theta_{j+2} - \theta_k - \gamma_{(j+2,k)}), \tag{4.9}$$
$$j = 1, 2, \ldots, nbHouse - 1$$

$$Q_{G_j} - Q_{L_j} = \sum_{k=j+1}^{j+3} |Y_{(j+2,k)}||V_{j+2}||V_k| \sin(\theta_{j+2} - \theta_k - \gamma_{(j+2,k)}), \tag{4.10}$$
$$j = 1, 2, \ldots, nbHouse - 1$$

$$P_{G_j} - P_{L_j} = \sum_{k=j+1}^{j+2} |Y_{(j+2,k)}||V_{j+2}||V_k| \cos(\theta_{j+2} - \theta_k - \gamma_{(j+2,k)}), \tag{4.11}$$
$$j = nbHouse$$

$$Q_{G_j} - Q_{L_j} = \sum_{k=j+1}^{j+2} |Y_{(j+2,k)}||V_{j+2}||V_k| \sin(\theta_{j+2} - \theta_k - \gamma_{(j+2,k)}), \tag{4.12}$$
$$j = nbHouse$$

$$V^{\min} \leq |V_i| \leq V^{\max}, \quad i = 2, 3, \ldots, N \tag{4.13}$$

$$0 \leq P_{G_j} \leq P_{G_j}^{\max}, \quad j = 1, 2, \ldots, nbHouse \tag{4.14}$$

$$0 \leq \sqrt{P_{G_j}^2 + Q_{G_j}^2} \leq S_j^{\max}, \quad j = 1, 2, \ldots, nbHouse \tag{4.15}$$

$$-\frac{\sqrt{1 - (\cos\varphi)_{\min}^2}}{(\cos\varphi)_{\min}} P_{G_j} \leq Q_{G_j} \leq \frac{\sqrt{1 - (\cos\varphi)_{\min}^2}}{(\cos\varphi)_{\min}} P_{G_j}, \quad j = 1, 2, \ldots, nbHouse \tag{4.16}$$

4.3.2 Extension to the time-variant case

In the time-variant case, the parameters P_{L_j}s, Q_{L_j}s and the $P_{G_j}^{\max}$s are not constant anymore.

One straightforward way to extend the logic presented in the previous paragraph to this time-variant case would be to solve the optimization problem presented in the previous subsection every time the parameters of the system change, so as to refresh the modulation orders.

However, it may technically unrealistic to recompute the modulation orders every time the parameters change, especially given the fact that some of them, e.g. the $P_{G_j}^{\max}$s, may evolve continuously during periods of the day. A more realistic approach would be to suppose that parameters are measured every Δt seconds and to recompute the orders every time a new set of measurements is available.

Let us now discuss how this time discretization influences the solution computed. Subsequently, the discrete instants $0, 1, 2, \ldots, t, t+1$ are used to refer to the time at which the measurements are taken. Naturally, the real-time between two successive discrete-time instants is equal to Δt seconds.
Let t_{delay} be the time required for measuring the parameters, sending them to the centralized controller, solving the optimization problem, sending the modulation orders to the inverters and applying these orders. First, let us assume that t_{delay} is arbitrarily small. In such a context, the value of the modulation orders will be refreshed at the beginning of the time interval $]t, t+1]$ and stay constant for the rest of the interval. It is only for the very beginning of the time interval that the modulation orders can be considered as being optimal with respect to the value of the parameters. Afterwards, their quality may decrease since the value of the parameters of the system evolve with time. There may even be periods during this time interval where the modulation orders lead to a system that violates the constraints. Obviously, the shorter the value of Δt, (i) the more likely the suboptimality incurred due to the time discretization will be small (ii) the smaller the violation of the constraints are likely to be. Now suppose that t_{delay} cannot be considered as being arbitrarily small. This would even worsen the suboptimality of the scheme and increase the chances that the constraints are seriously violated, especially if the parameters evolve significantly over a period of t_{delay} seconds. One way to mitigate these problems would be to solve the optimization problem with predicted values for the parameters, rather than with the values corresponding to the last set of measurements. For example, once receiving a new set of measurements, the controller would start by predicting their values t_{delay} seconds afterwards and then inject these predicted values into its optimization

problem to compute its modulation orders. Note that predicting these values may not be an easy task since, for example, the evolution of the load at the house level can depend on factors that cannot be easily modeled.

4.3.3 Simulation results

We report here results obtained on our problematic test system already studied in Chapter 2. We give in Table 4.1 the value of the parameters of the system and the optimal power flow. These are assumed not to vary with time.

Table 4.1: Optimal power flow data.

Nominal voltage	400 V
Line resistance	0.24 Ω/km
Line reactance	0.1 Ω/km
Number of houses	18
Distance between houses	50 m
Peak power production of PV panels ($S_j^{\max}$)	7 kW
Maximum active power available ($P_{G_j}^{\max}$)	7 kW
Minimum power factor of the PV inverters ($(\cos\varphi)_{\min}$)	0.8
House active power consumption (P_{L_j})	1 kW
House reactive power consumption (Q_{L_j})	0 kvar
Voltage limits ($V^{\min}$ and $V^{\max}$)	400 V ± 10%

We are here in a case where our control scheme (i) measures the value of the parameters (ii) sends them to the centralized controller which solves the optimization problem defined in Subsection 4.3.1 (iii) sends the modulation orders derived from the solution of this optimization problem to the inverters which implement them.

Note that in our simulations, we have used the *optimization toolbox* of MATLAB for computing the modulation orders.

Figure 4.1-top reports the voltages obtained after implementing the modulation orders. We clearly see that with these modulation orders, the voltages are driven within their limits. We also observe that after applying the modulation orders, the voltages

rise when going further into the feeder. For the last house, the voltage is equal to 1.1 p.u. Note that 1.1 is the upper limit on the voltages ($V^{\max}$).

Figure 4.1-bottom reports the modulation orders sent to every inverter. As we can see, the further we go into the feeder, the lower the values of P_{G_j} and Q_{G_j} are. Since $P_{G_j}^{\max}$ is the same for every house, that means that the controller curtails more the power that could be outputted by PV installations far from the MV/LV transformer than the power of installations located close to the MV/LV transformer. Observe also that the reactive power is always negative. This was expected since it is well-known that drawing reactive power from a network has for effect to lower its voltage. Note that the total amount of active power that had to be curtailed for reaching this new voltage profile is equal to 7.6 kW. This corresponds to a little bit more than the maximum power that can be outputted by a single PV installation (7 kW).

We finish this subsection by illustrating the benefits of having inverters which can modulate their reactive power output. For doing so, we have run again our optimization problem by constraining this time the Q_{G_j}s to be always equal to zero. The results are reported on Figure 4.2. The total amount of power curtailed is now equal to 20.2 kW. That is around three times the maximum power output of a single PV installations. Thanks to the reactive power compensation, it was possible to inject $20.2 - 7.6 = 12.6$ kW more into the network.

4.4 Towards fair centralized control schemes

In the previous section, we have reported simulation results for our centralized control scheme. In particular, we have shown in Section 4.3.3 that by applying the right modulation orders, our scheme was able to avoid voltage problems in our test system by curtailing only 7.6 kW of power. Table 4.2 gives the power curtailed at every house of the street. We observe that the last houses of the feeder have to curtail much more power than the first ones. As a result, the last houses of the feeder will earn less from their PV installations than the first ones. This may be considered as unfair since there is a priori no reason why a prosumer should pay more than another one to avoid problems on the distribution network.

One way to overcome this problem would be to meter the amount of energy every prosumer has to curtail due to this centralized control scheme and give him a fair compensation for the financial losses incurred. This compensation could for example be paid by increasing the distribution tariff. This may however be unfair to the

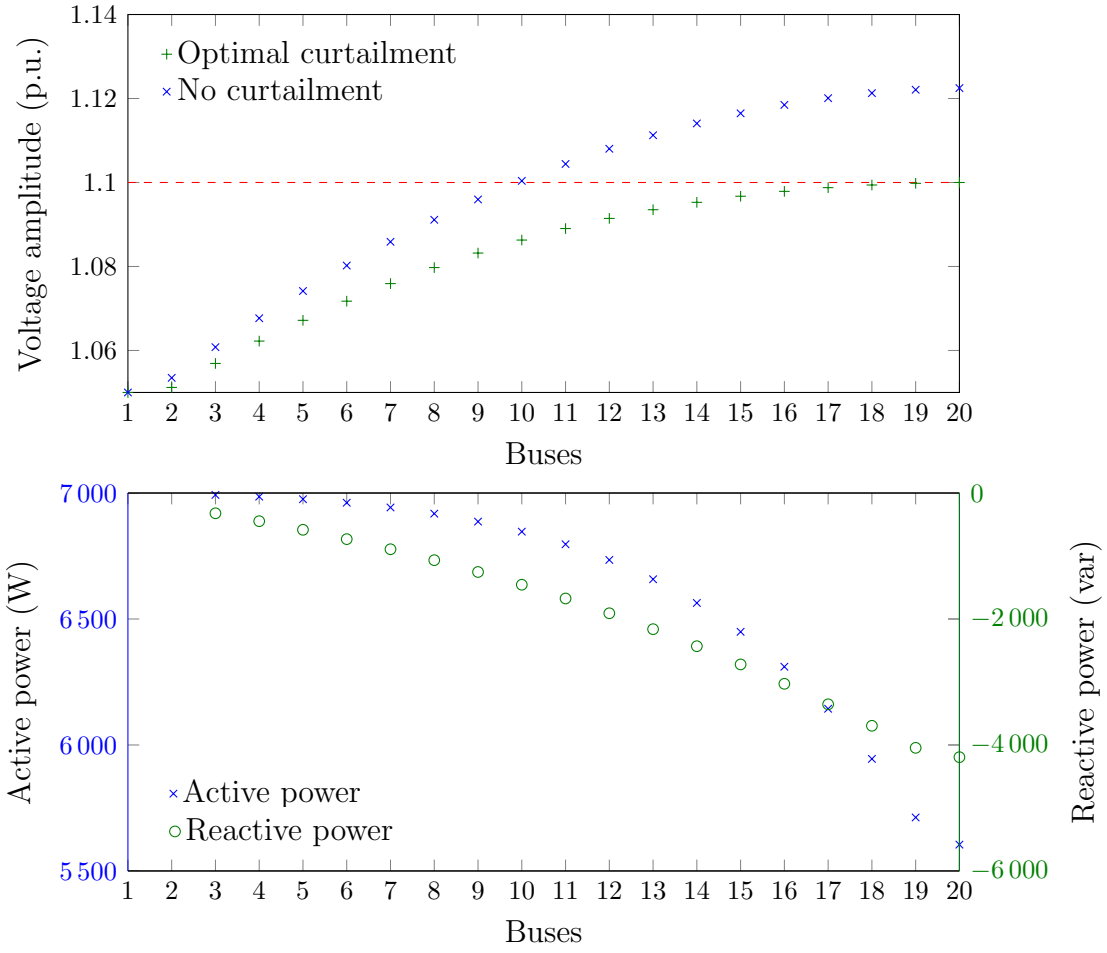

Figure 4.1: Results for the centralized control strategy. Figure-top: the blue crosses report the voltages when $P_{G_j} = P_{G_j}^{\max}$ and $Q_{G_j} = 0\ \forall j \in \{1, 2, \ldots, nbHouse\}$. The green plus symbols report the voltages obtained after applying the values of the P_{G_j}s and the Q_{G_j}s computed by the centralized controller. Figure-bottom: the green bullets give the values of the Q_{G_j}s and the blue crosses the values of the P_{G_j}s.

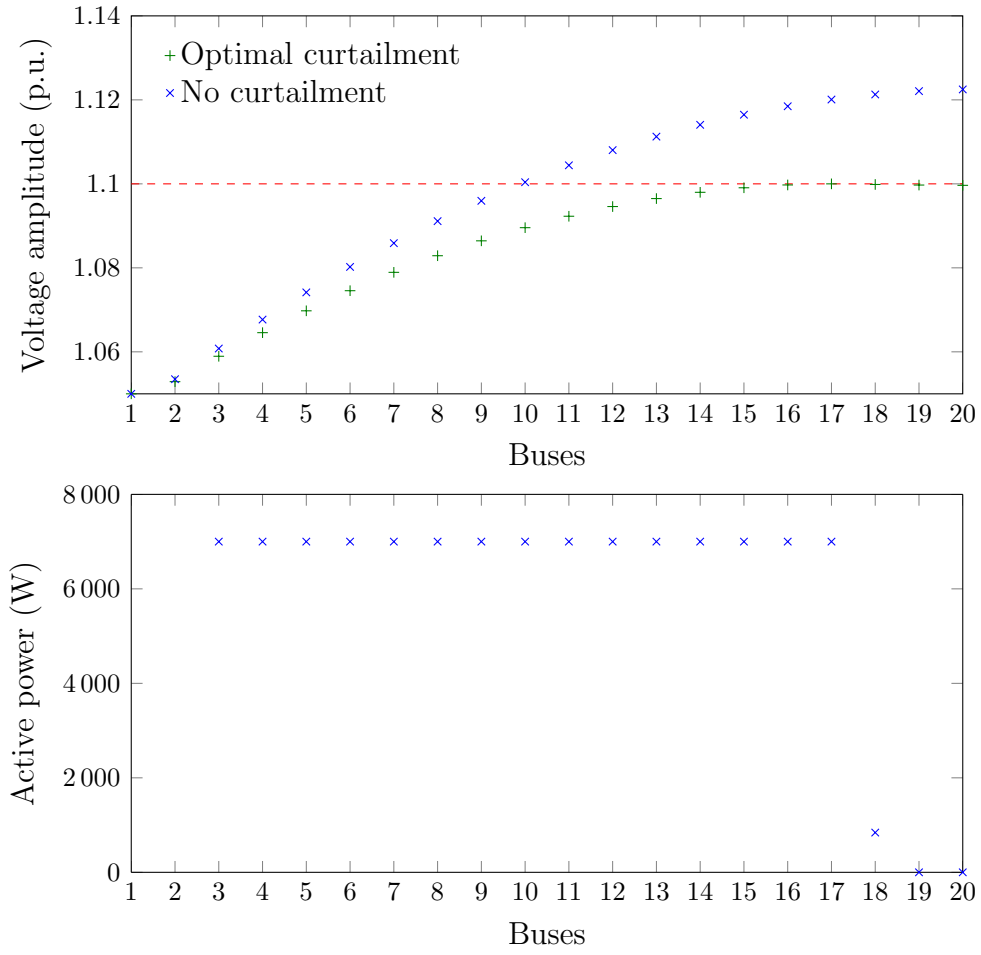

Figure 4.2: Optimal power flow as defined in Program 3, without reactive power modulation, when $P_{G_j}^{\max} = 7000$ W for every PV unit.

Table 4.2: Power curtailed for each house.

House	Power curtailed (W)	House	Power curtailed (W)
1	8	10	266
2	14	11	342
3	25	12	436
4	39	13	551
5	57	14	689
6	82	15	856
7	113	16	1055
8	153	17	1288
9	203	18	1395
Total			**7574**

people who do not own PV installations since they would have to pay for problems that they do not cause. Another solution would be to make only the owners of the PV installations pay for these compensation costs. Note that sharing these compensation costs equally among the owners of PV installations may however not be that fair. Indeed, prosumers having small PV installations will end up paying the same amount of money as people having large ones. It would therefore be preferable to share the compensation costs among PV owners according to the size of their installation.

Another way to address this fairness problem would be to rely on a scheme that would be intrinsically fair, rather than on a compensation mechanism for correcting its lack of fairness. For example, a scheme that would curtail the same amount of power for every PV installation or, even better, that would curtail the same percentage of power in every PV installation, could be considered as fair. For building such a scheme, we propose to add a new set of equality constraints in the optimisation problem proposed in Section 4.3 so as to ensure that every house j has to curtail the same fraction of its $P_{G_j}^{\max}$. This set of equality constraints corresponds to (4.18) of the Program 4 given hereafter.

Program 4: Fair OPF

$$\min_{P_G^{tot},P_{G_j},Q_{G_j},|V_i|,\theta_i} \quad \sum_{j=1}^{nbHouse} P_{G_j}^{\max} - P_G^{tot} \tag{4.17}$$

subject to

$$P_{G_j} = P_G^{tot}\frac{P_{G_j}^{\max}}{\sum_{k=1}^{nbHouse} P_{G_k}^{\max}}, \quad j = 1,2,\ldots,nbHouse \tag{4.18}$$

$$0 = \sum_{k=1}^{3} |Y_{(2,k)}||V_2||V_k|\cos(\theta_2 - \theta_k - \gamma_{(2,k)}) \tag{4.19}$$

$$0 = \sum_{k=1}^{3} |Y_{(2,k)}||V_2||V_k|\sin(\theta_2 - \theta_k - \gamma_{(2,k)}) \tag{4.20}$$

$$P_{G_j} - P_{L_j} = \sum_{k=j+1}^{j+3} |Y_{(j+2,k)}||V_{j+2}||V_k|\cos(\theta_{j+2} - \theta_k - \gamma_{(j+2,k)}), \quad j = 1,2,\ldots,nbHouse-1 \tag{4.21}$$

$$Q_{G_j} - Q_{L_j} = \sum_{k=j+1}^{j+3} |Y_{(j+2,k)}||V_{j+2}||V_k|\sin(\theta_{j+2} - \theta_k - \gamma_{(j+2,k)}), \quad j = 1,2,\ldots,nbHouse-1 \tag{4.22}$$

$$P_{G_j} - P_{L_j} = \sum_{k=j+1}^{j+2} |Y_{(j+2,k)}||V_{j+2}||V_k|\cos(\theta_{j+2} - \theta_k - \gamma_{(j+2,k)}), \quad j = nbHouse \tag{4.23}$$

$$Q_{G_j} - Q_{L_j} = \sum_{k=j+1}^{j+2} |Y_{(j+2,k)}||V_{j+2}||V_k|\sin(\theta_{j+2} - \theta_k - \gamma_{(j+2,k)}), \quad j = nbHouse \tag{4.24}$$

$$V^{\min} \le |V_i| \le V^{\max}, \quad i = 2,3,\ldots,N \tag{4.25}$$

$$0 \le P_{G_j} \le P_{G_j}^{\max}, \quad j = 1,2,\ldots,nbHouse \tag{4.26}$$

$$0 \le \sqrt{P_{G_j}^2 + Q_{G_j}^2} \le S_j^{\max}, \quad j = 1,2,\ldots,nbHouse \tag{4.27}$$

$$-\frac{\sqrt{1-(\cos\varphi)_{\min}^2}}{(\cos\varphi)_{\min}}P_{G_j} \le Q_{G_j} \le \frac{\sqrt{1-(\cos\varphi)_{\min}^2}}{(\cos\varphi)_{\min}}P_{G_j}, \quad j = 1,2,\ldots,nbHouse \tag{4.28}$$

If we run this optimization problem on our problematic test system, we get the solution reported on Figure 4.3.

As can be seen, the value of P_{G_j} is the same for all the houses, which is normal since $P_{G_j}^{\max}$ is the same $\forall j$. P_{G_j}s are equal to 6450 W, which leads to a total of $18 \cdot (7000 - 6450)$ W $= 9.9$ kW curtailed. Note that in the case of an *unfair* centralized control scheme, "only" 7.6 kW had to be curtailed. This shows that control schemes that are intrinsically fair tend however to curtail significantly more power.

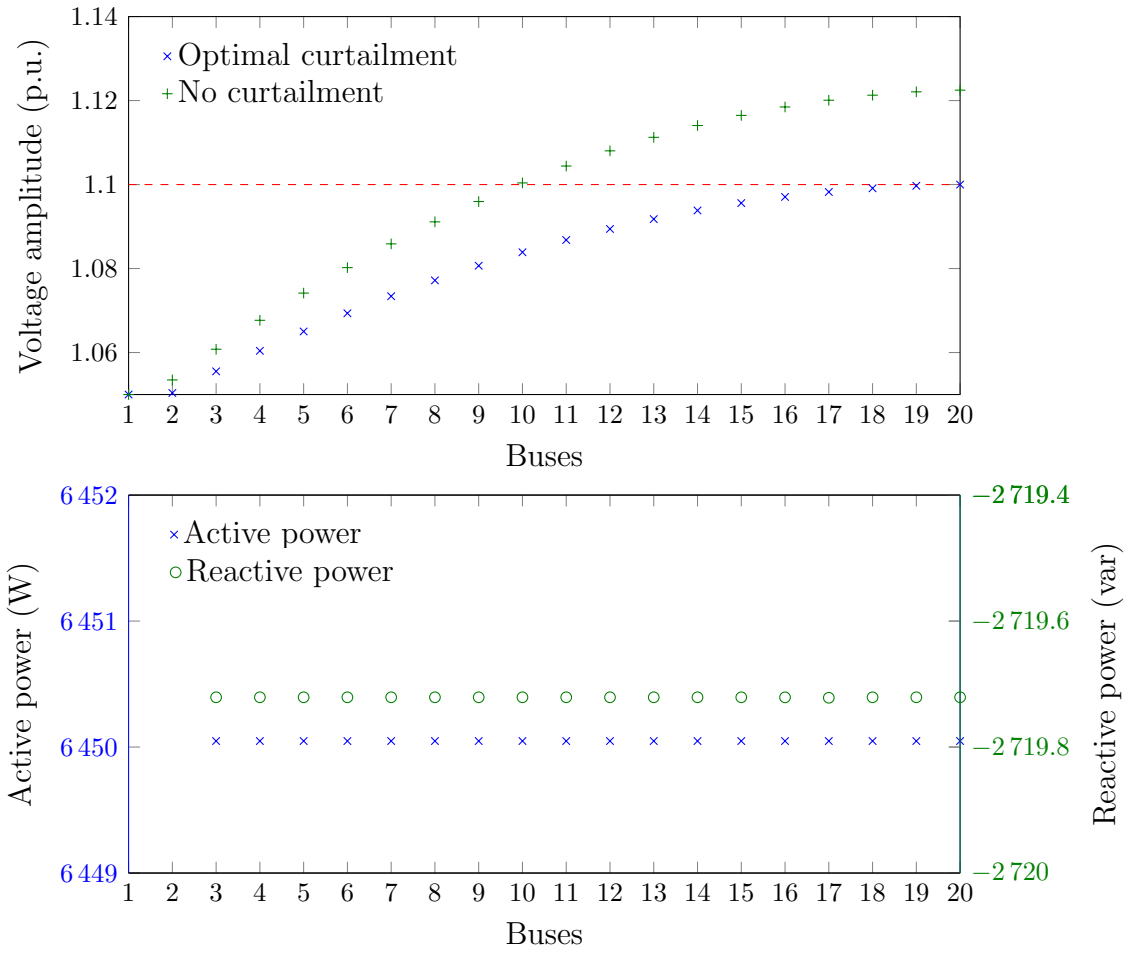

Figure 4.3: Fair optimal curtailment of the PV panels, with use of reactive power modulation.

Chapter 5

Decentralized solution

In this chapter, we study distributed control based approaches to suppress overvoltages caused by PV installations in low-voltage distribution networks. We focus on distributed controllers for which every inverter is controlled based only on local information and that do not require a model of the low-voltage network. The first distributed controller that will be studied modulates only the active power. The second modulates both the active and reactive power. Simulation results compare the performance of these distributed schemes with a centralized one.

5.1 Introduction

In the previous chapter, we have proposed centralized controllers to suppress overvoltages in low-voltage distribution networks. One of the main shortcomings of these controllers is their cost of implementation and maintenance. They indeed require to build and maintain a costly communication infrastructure between the houses and the centralized controllers. This infrastructure was required (i) for sending to the centralized controller the load consumption of the houses and the maximum power the PV installations can inject into the network (ii) for sending from the centralized controller to the inverters the modulation orders. Additionally, they also require a detailed model of the low-voltage network that may be expensive to get.

Therefore, it would be interesting to design other types of control schemes that would be much cheaper. Ideally, these schemes should not rely on an expensive communication architecture and be able to work without even knowing a detailed

model of the low-voltage network. In that mindset, we propose in this chapter distributed controllers that do not exploit any model of the low-voltage network and for which every inverter is controlled based only on local information. These controllers work by adjusting in an iterative way the active and/or the reactive power of a inverter, based on the effect of the past adjustments on the local voltage.

In Section 5.2, we will formally introduce the general class of distributed controllers we focus on, and the different elements that will be used later for studying their properties. In Section 5.3, we will study a first distributed controller that modulates only the active power of the inverters. Section 5.4 describes and analyses a second distributed control scheme that works by modulating both the active and reactive power of the inverters.

5.2 The distributed logic

In the distributed case, PV inverters are controlled by a smart entity, formally called agent. An agent is an entity that has been given power of decision. Those agents evolve in an environment: the low voltage distribution network modeled in Chapter 2. They can sense this environment and take actions accordingly. The agents are assumed to know local information about their environment (local voltage and maximum power the solar panels can produce). Their actions are the modulation orders they can send to the PV inverters, i.e. they can set the particular value of active and reactive power that the PV inverter must supply to the grid.

The agents are discrete processes, in opposition to continuous ones. We will consider here only agents that have been designed so as to refresh the value of their actions every Δt seconds . We will assume that they sense the network every Δt seconds and that there is no delay between sensing and acting. Sensing, computing, and acting are done instantaneously.

Formally, the intelligence of an agent is defined as a function whose arguments are the history of voltages at the bus where the PV inverter delivers power, and the history of active and reactive power supplied by the PV panels. One might also add to this list the history of the maximum power that the PV panels can supply given current sunlight. This function outputs the amount of active and reactive power that the PV inverter associated to that agent must supply to the grid. Let agent j be the agent that controls the PV inverter installed on house j and let $V_{j+2,[k]}$, $P^{\max}_{G_j,[k]}$ denote the $k+1$ first measurements of the voltage at house j and of the maximum

power that can be supplied without curtailment, respectively. We will focus here on a distributed logic where the setting for the active and reactive power imposed by agent j after its $k+1$ first sets of measurements is computed based on a function h generically defined as follows:

$$(P_{G_j,k}, Q_{G_j,k}) = h\left(V_{(j+2),[k]}, P_{G_j,[k-1]}, Q_{G_j,[k-1]}, P^{\max}_{G_j,[k]}\right) . \tag{5.1}$$

Let t and $t+1$ denote two discrete instants separated by Δt seconds. Now that the logic of every individual agent has been defined, the distributed solution is fully defined once we know in an interval $[t, t+1]$ the exact time at which an agent j is going to act.

This time could be chosen so as it would be the same for all the agents. In such a context, the agents would be synchronized. Synchronizing agents may however be difficult to achieve on a technical point of view, since it would imply that they share a common time reference.

In all the simulation results reported here, we will not assume that they are synchronized and the order in which they select their actions has been drawn at random.

To analyze the quality of such a distributed control scheme, several criteria can be used.
First, by assuming that the $P^{\max}_{G_j}$ are constant, we may want to understand whether the scheme converges or not to a set of control actions. If yes, it would also be worth analyzing the quality of the actions it converges to, with respect to the solution outputted by the centralized solution.
Second, it would also be worth understanding better the finite time properties of the distributed scheme. Indeed, even if it converges towards an optimal solution, here defined as being the centralized solution, nothing guarantees that the scheme is good. Indeed, the scheme may lead for example to so much energy curtailed before reaching this convergence point or so many severe violations of the constraints that it may actually be of very poor quality. Note that the sum of the energy curtailed after t discrete time steps grows linearly with the sampling period Δt. Therefore, for example, in a context where the scheme takes too long before converging towards a near-optimal solution, it may be worth decreasing the value of Δt.
Third, studying the properties of the control scheme when the loads and the maximum power that can be injected by the PV panels vary with time may also be interesting.

In Section 5.3, we will propose a function h that only modulates the active power. In Section 5.4, we will propose a function h that modulates both the active and reactive power.

5.3 Active power modulation

In the first subsection (Subsection 5.3.1), we will present the distributed logic we are going to use for modulating the active power. In the second one (Subsection 5.3.2), we will report on simulation results obtained by running the resulting distributed controller on our test network.

5.3.1 Distributed control logic

The design of the distributed logic will be based on the analysis of the optimal solution for our problematic test network and of the operating points in the neighborhood of the optimal solution. Let us recall Figure 4.2 from Chapter 4 which displays the centralized optimal solution when only active power can be modulated and all PV units have a $P_G^{\max}$ equal to 7 kW.

We first have a look at the constraints that are active at the optimal solution. We remind that for every house j, three inequalities were constraining the solution. In a context where there is only active power modulation, as it is the case here, these inequalities are:

$$V^{\min} \leq |V_{j+2}| \leq V^{\max} \tag{5.2}$$
$$0 \leq P_{G_j} \leq P_{G_j}^{\max} \tag{5.3}$$
$$0 \leq P_{G_j} \leq S_j^{\max} \tag{5.4}$$

After running our centralized scheme, we observe as active constraints:

- the upper constraints on the power generated by houses 1 to 15 (buses 3 to 17),
- the upper voltage limit constraint for bus 17.

Now, let us try to understand how the solution varies by changing the value of P_{G_j} for a given j. For every $j \in \{1, 2, \ldots, 17\}$, we observe that by decreasing P_{G_j}, the voltage at node j decreases and that no constraints are violated. For every house j that has

not yet reached its maximal power output (i.e., $P_{G_j}^{\max}$) increasing P_{G_j} leads to a value of V_{j+2} which is larger than $V^{\max}$. Let us assume now that all the houses, except the house j', have a value of P_{G_j} which is equal to the value given by the centralized scheme. Let us also assume that $P_{G_{j'}}$ is smaller than $P_{G_{j'}}^{\max}$ and that the distributed control scheme refreshes at every Δt the value of $P_{G_{j'}}$ according this simple rule: if the voltage at this house is lower than $V^{\max}$, increase if physically possible its power output by ϵ, otherwise decrease it by ϵ. Based on the above observations, it is reasonable to conjecture that such a control scheme would drive $P_{G_{j'}}$ to a small neighborhood of the value given by the centralized control scheme, provided that ϵ is small enough.

This naturally calls for a function h that would set the value of $P_{G_j,k}$ equal to $P_{G_j,k-1} + \epsilon$ if $V_{j+2,k} \leq V^{\max}$ and to $P_{G_j,k-1} - \epsilon$ if $V_{j+2,k} > V^{\max}$, provided of course that $P_{G_j,k}$ always satisfies inequality constraint (5.3).

Note that this function h depends on a parameter ϵ. Intuitively, the further $V_{j+2,k}$ is from $V^{\max}$, the larger this parameter should be. This is why taking this value proportional to the distance between $V_{j+2,k}$ and $V^{\max}$ may be reasonable. Note that simulation results have shown that such a function h may however lead to slight voltage violations. This is why in the version of the distributed scheme that we will test, we will not take a value of ϵ proportional to the distance between $V_{j+2,k}$ and $V^{\max}$ but well to the distance between $V_{j+2,k}$ and V^{ref}, with $V^{ref} < V^{\max}$.

The detailed tabular version of the distributed logic adopted for an agent is given in Program 5. This program takes as arguments $P_{G_j,k-1}$, $P_{G_j,k}^{\max}$ and $V_{j+2,k}$, and outputs the value of for $P_{G_j,k}$ and $Q_{G_j,k}$. Constraint (5.4) is always satisfied, since it is assumed that the PV units are designed so that the PV inverters are able to supply the peak generated power, i.e. $P_{G_j,k}^{\max} \leq S^{\max}$.

Program 5: Logic for agent j to modulate active power

- Compute the error between the current voltage and the reference voltage.

$$e_{V_{j+2},k} = V^{ref} - V_{j+2,k} \tag{5.5}$$

- Find the next amount of active power to supply according to the proportional control law (5.6).

$$P_{G_j,k} = \max\left(0, \min\left(P^{\max}_{G_j,k}, P_{G_j,k-1} + K_p\, e_{V_{j+2},k}\right)\right) \tag{5.6}$$

$$Q_{G_j,k} = 0 \tag{5.7}$$

  Equation (5.6) ensures that $P_{G_j,k}$ is within limits. If it is negative, it is brought back to zero and if it is superior to $P^{\max}_{G_j,k}$, it is brought back to this limit.

5.3.2 Simulation results

We start this section by discussing our experimental protocol. Afterwards, we will describe a run of our test network system when controlled by our distributed algorithm. Finally, we will carefully analyze how the distributed scheme compares with the centralized scheme.

Experimental protocol

The experiments will be carried out on the test system described in Chapter 2. The network data are the same as those used for the centralized solution (Table 4.1). We will suppose in our experiments that during the first Δt seconds, the value of $P^{\max}_{G_j}$ is the same for all the houses and equal to 2000 W. Note that for such values of $P^{\max}_{G_j}$, no voltage problems exist on the network. We will also assume that at time $t = 0$ — the first discrete time step — all the agents have a value of P_{G_j} equal to $P^{\max}_{G_j}$. After Δt seconds, the value of $P^{\max}_{G_j}$ $\forall j$ is increased to 7000 W.

Note that during the Δt seconds of every time interval $[t, t+1]$, every agent will sense the network, compute its control action and apply it on the network. The order according to which the agents update their actions in a time interval has been

chosen randomly and is the following: first we have the agent 16, followed by agent 8, agent 10, agent 3, agent 9, agent 5, agent 13, agent 18, agent 17, agent 1, agent 11, agent 6, agent 15, agent 4, agent 7, agent 14, agent 12, and, finally, agent 2. We have also ensured that no agent updates its actions at a time equal to a multiple of Δt.

The simulations will be stopped after $8\Delta t$ seconds.

Note that our distributed control scheme depends on two parameters: the reference voltage V^{ref} and the proportionality constant K_p. The values of these parameters have been chosen — with little tuning — equal to 1.08 and 0.5, respectively.

Behavior of the test network

Figure 5.1 reports the evolution of the voltages at the different buses of the system and Figure 5.2 displays the evolution of the active power P_{G_j} generated by each PV unit after a multiple of Δt seconds.

The first thing that can be noticed is that during the first Δt seconds, nothing changes in the network. This was expected since (i) at time $t = 0$, all the agents have a value of P_{G_j} equal to $P_{G_j}^{\max}$, (ii) when the set of control actions does not lead to voltage problems (as it is the case here), it is also a sationary point of our distributed control scheme. After Δt seconds, the value of $P_{G_j}^{\max}$ is set to 7000 W for every PV installation. As a result, the agents start increasing their value of P_{G_j}. As we can see, this leads to a voltage rise. Voltages at the buses located at the end of the street even reach a value close to 1.09. After some time, we observe however that those voltages go down to 1.08, the value of V^{ref} in our control scheme.

Comparison with the centralized control scheme

In the previous section, we have seen that our distributed control scheme was converging after a few discrete time steps towards a stationary solution. We have also seen that during the transient period leading to this stationary solution, the upper limit on the voltages, which is equal to 1.1 p.u., was never violated. Now we want to establish how the distributed control scheme compares to the centralized one. Figure 5.3 reports the voltages and the power output that are obtained with the centralized solution and with the solution the distributed scheme converges to. Note that the value of the upper voltage limit in the centralized optimal power flow has

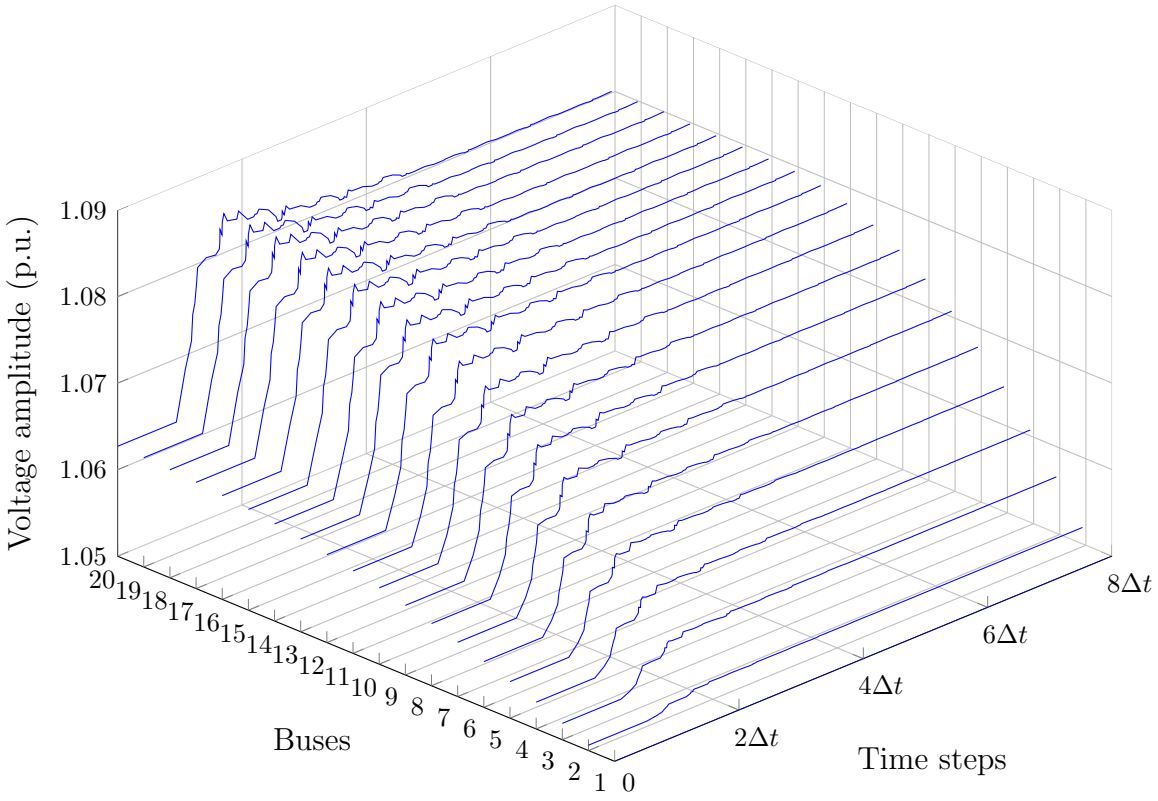

Figure 5.1: Voltage evolution for each bus when $P_{G_j}^{\max}$ $\forall j$ increases from 2000 W to 7000 W at time equal to Δt seconds.

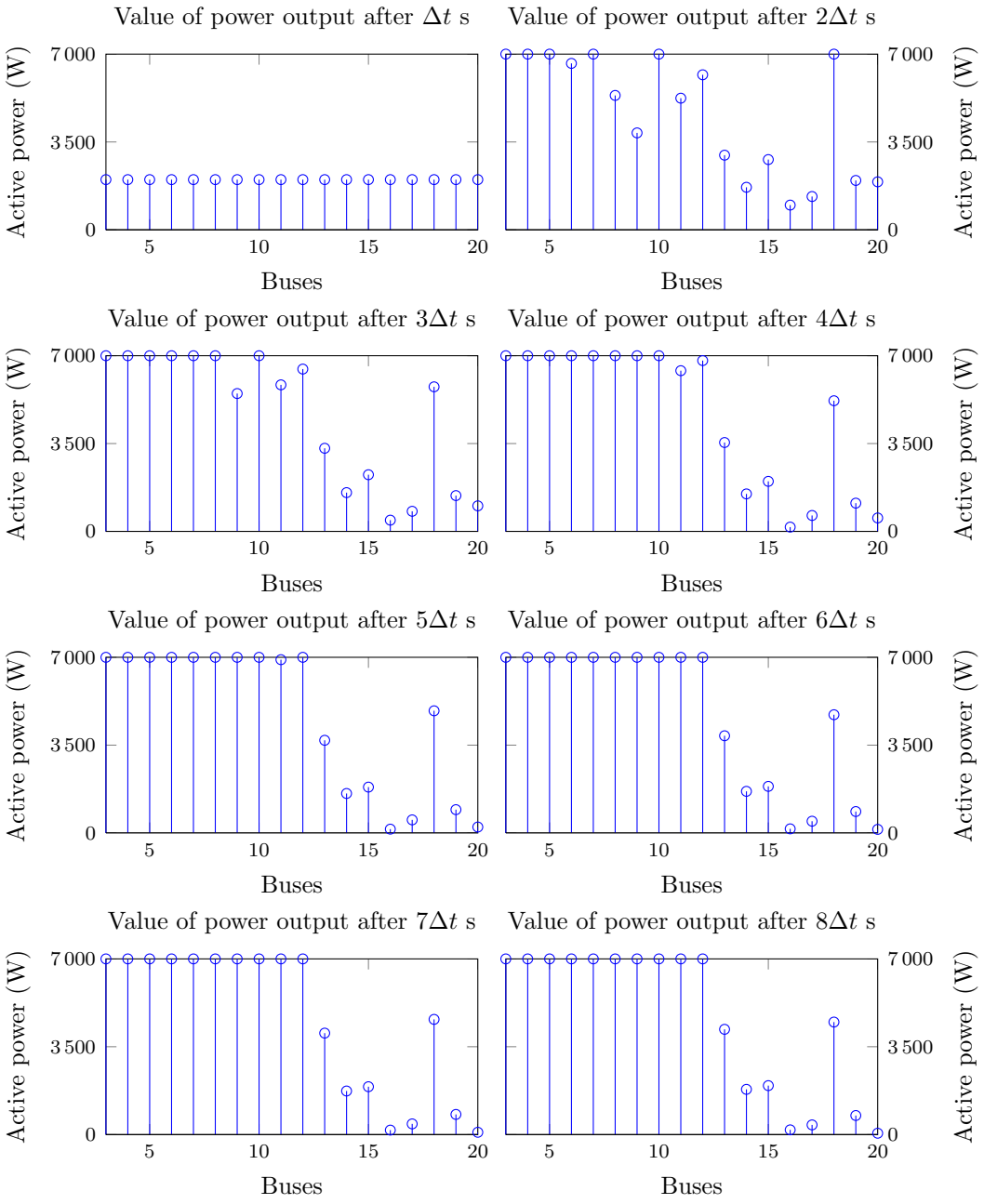

Figure 5.2: Evolution of the power generated by each PV unit.

been lowered to V^{ref} (1.08 p.u.) to allow a more meaningful comparison between the two schemes. As we can see, the voltage profiles are very similar. However, more differences can be observed when it comes to values of P_{G_j}. In particular, while for the centralized solution P_{G_j} strictly decreases after $j = 11$ (bus 13), it is not the case with the distributed solution. For example, the value of $P_{G_{16}}$ (bus 18) is significantly higher than the value of $P_{G_{15}}$ and $P_{G_{17}}$ (resp. bus 17 and 19). Table 5.1 reports the values of the power curtailed by both schemes. By processing the results of this table, we can notice that the distributed scheme only curtails 0.957% more power than the centralized control scheme.

Table 5.1: Comparison between power curtailed in the centralized case and in the distributed case, after convergence.

House	Power curtailed (W)		House	Power curtailed (W)	
	Centralized	Distributed		Centralized	Distributed
1	0	0	10	0	0
2	0	0	11	0	2810
3	0	0	12	1670	5200
4	0	0	13	6300	5050
5	0	0	14	6640	6810
6	0	0	15	6740	6610
7	0	0	16	6790	2520
8	0	0	17	6810	6240
9	0	0	18	6820	6950
Total	Centralized	**41800 W**		Distributed	**42200**

Note that we are not really interested by the amount of power curtailed by our distributed control in "asymptotic conditions" but well by the amount of energy it curtails during a period of time. Computing this amount of energy implies choosing a value for Δt. Here, we have chosen this value equal to one minute and reported the amount of energy curtailed from minute 1 to minute 8. For the centralized scheme, we have assumed that the values of the P_{G_j}s were optimal during the whole time interval. Table 5.2 reports the amount of energy curtailed for both schemes. By processing the results of this table, we see that the distributed scheme curtails 1.56% more energy than the centralized one. Note that if we keep constant the time period

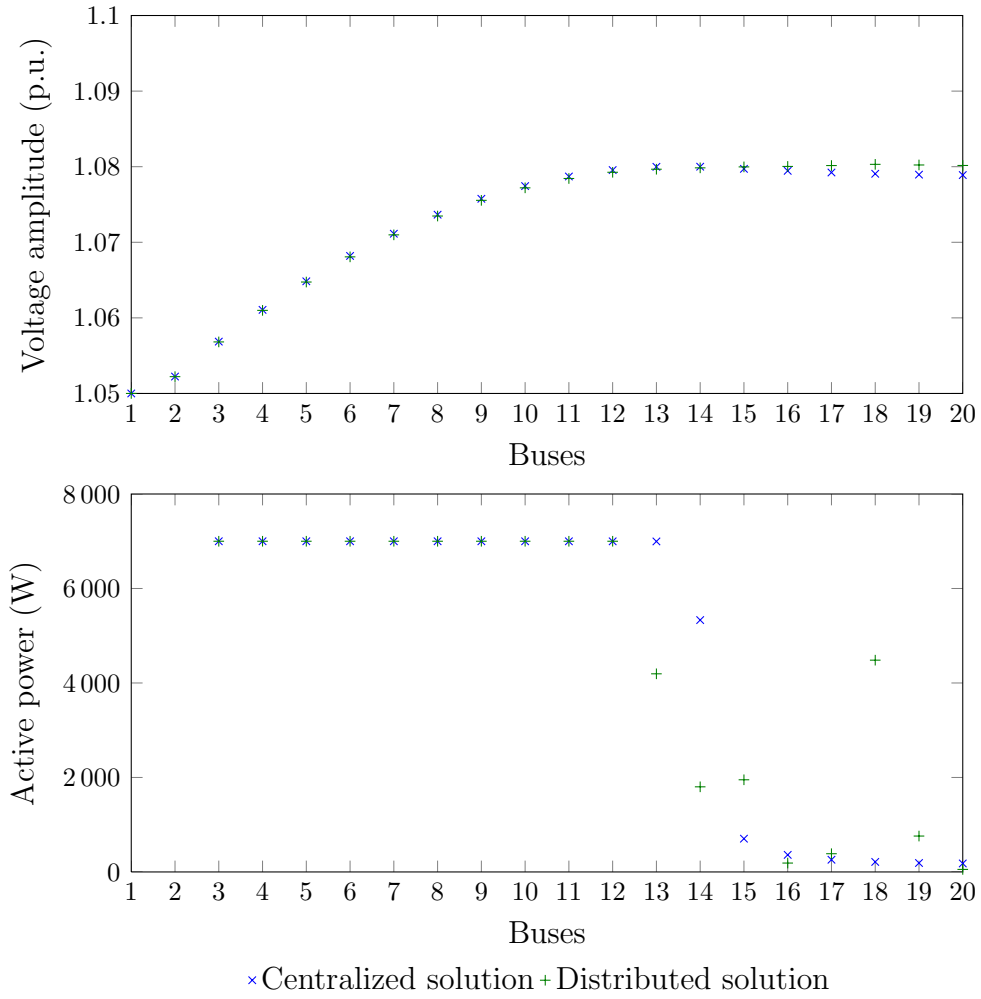

Figure 5.3: Centralized solution and convergence point of the distributed solution when $P_{G_j}^{\max} = 7$ kW $\forall j$.

over which we compute the amount of energy curtailed and decrease the value of Δt, this pourcentage is going to decrease to 0.957, the percentage of additional curtailed power by the stationary solution.

Table 5.2: Comparison between electrical energy curtailed in the centralized case and in the distributed one over the period $[1\text{ min}, 8\text{ min}]$ when $\Delta t = 1$ min.

House	Energy curtailed (kWh)		House	Energy curtailed (kWh)	
	Centralized	Distributed		Centralized	Distributed
1	0	0	10	0.000199	0.0258
2	0	0	11	0.000397	0.343
3	0	0	12	0.167	0.538
4	0	0.00615	13	0.63	0.489
5	0	0	14	0.664	0.665
6	0	0.0274	15	0.674	0.63
7	0	0.0774	16	0.679	0.164
8	0.0001	0	17	0.681	0.582
9	0.000133	0.0601	18	0.682	0.634
TOTAL	Centralized	**4.1774**		Distributed	**4.2427**

5.4 Active power and reactive power modulation

In Section 5.4.1, we will present our distributed control logic for modulating both the active and reactive power. Afterwards, in Section 5.4.2, we will assess the performance of our distributed control scheme on the test network presented in Chapter 2.

5.4.1 Distributed control logic

As first step for building a logic for our distributed agents, we will use our knowledge of the physics of the system. It tells us that the more the voltage grows, the more it is preferable to withdraw reactive power from the network to counteract this rise.

In that mindset, we have chosen to develop a distributed control logic that constraints agent j to take, at step k, actions $P_{G_j,k}$ and $Q_{G_j,k}$ that lead to a power factor $\cos\varphi_{j,k}$ which is such that:

1. It is equal to one when the voltage at node j is sufficiently small. The voltage of a node will be considered sufficiently small, when it is lower than V^{var} where V^{var} is a parameter of our algorithm. This parameter has been chosen equal to 1.065 p.u. in our simulations.
2. It grows linearly with V_{j+2} once $V_{j+2} > V^{var}$, in a way such that $(\cos\varphi)_{\min}$ is reached when V_{j+2} is equal to V^{ref}. V^{ref} is another parameter of our algorithm. It should be chosen slightly below $V^{\max}$. Indeed, as we will see in our simulations, our distributed scheme leads to voltages which are slightly above V^{ref}. This parameter is chosen equal to 1.08 p.u. in our experiments.
3. It is always equal to $(\cos\varphi)_{\min}$ once $V_{j+2} > V^{ref}$.

More specifically, we constraint $P_{G_j,k}$ and $Q_{G_j,k}$ to correspond to a value of $\cos\varphi_{j,k}$ equal to:

$$\cos\varphi_{j,k} = 1 \qquad \text{if } V_{j+2,k} \leq V^{var} \tag{5.8}$$

$$\cos\varphi_{j,k} = \frac{(\cos\varphi)_{\min} - 1}{V^{ref} - V^{var}}(V_{j+2,k} - V^{var}) + 1 \qquad \text{if } V^{var} < V_{j+2,k} < V^{ref} \tag{5.9}$$

$$\cos\varphi_{j,k} = (\cos\varphi)_{\min} \qquad \text{if } V_{j+2,k} \geq V^{ref} \tag{5.10}$$

Note that, since we constraint $P_{G_j,k}$ and $Q_{G_j,k}$ to correspond to a well-specified value of $\cos\varphi_{j,k}$, we just need to build a logic for computing $P_{G_{j,k}}$ to have a fully specified control logic for agent j. Indeed, the value of $Q_{G_j,k}$ can be computed from $\cos\varphi_{j,k}$ and $P_{G_j,k}$ according to (5.11).

$$Q_{G_j,k} = -\frac{\sqrt{1 - \cos^2\varphi_{j,k}}}{\cos\varphi_{j,k}} P_{G_j,k} \tag{5.11}$$

To one value of $\cos\varphi$ can correspond two values for reactive power, one positive and the other one negative. Since our wish is to limit voltage rise, reactive power is drawn from the network, and hence it is negative.

The logic that we have adopted for computing $P_{G_j,k}$ is rather simple. If $P_{G_j,k-1}$ is smaller than $P^{\max}_{G_j,k}$, we try to increase the value of the active power injected by agent j at iteration k, with respect to iteration $k-1$. To compute the magnitude of this increase, we exploit a linear model relating the variations of active and reactive power

injected by agent j to the variation of voltage ΔV_{j+2}. This model is represented by the following equation:

$$\Delta V_{j+2,k} = K_{P_j}\left(P_{G_j,k} - P_{G_j,k-1}\right) + K_{Q_j}\left(Q_{G_j,k} - Q_{G_j,k-1}\right) \tag{5.12}$$

where K_{P_j} and K_{Q_j} are two parameters. They approximate the derivatives of the voltage V_{j+2} with respect to P_{G_j} and Q_{G_j}, respectively. We explain later in this section how these coefficients will be learned on-line.

Based on this model, we compute the value of P_{G_j} leading to a value of V_{j+2} equal to V^{ref} and set temporary $P_{G_j,k}$ to this value. By doing elementary calculations, we have that this temporary value for $P_{G_j,k}$ is given by:

$$P_{G_j,k} = \frac{\Delta V_{j+2,k} + K_{P_j} P_{G_j,k-1} - K_{Q_j} Q_{G_j,k-1}}{\left(K_{P_j} - K_{Q_j}\frac{\sqrt{1-\cos^2\varphi_{j,k}}}{\cos\varphi_{j,k}}\right)} \tag{5.13}$$

with $\Delta V_{j+2,k}$ equal to $V^{ref} - V_{j+2,k}$.

Afterwards, we check whether this temporary value for $P_{G_j,k}$ satisfies the following constraints:

$$0 \leq \quad P_{G_j,k} \quad \leq P_{G_j,k}^{\max} \tag{5.14}$$

$$0 \leq \quad \sqrt{P_{G_j,k}^2 + Q_{G_j,k}^2} \quad \leq S_j^{\max} \tag{5.15}$$

If yes, this temporary value for $P_{G_j,k}$ becomes the value of the active power of inverter j at instant k. If not, we compute the largest value of $P_{G_j,k}$ satisfying the above written inequalities and set $P_{G_j,k}$ to this value. Note that since $P_{G_j,k}$ and $Q_{G_j,k}$ satisfy equation (5.11), the two above-written inequalities can be expressed solely as a function of $P_{G_j,k}$:

$$0 \leq \quad P_{G_j,k} \quad \leq P_{G_j,k}^{\max} \tag{5.16}$$

$$0 \leq \quad P_{G_j,k} \quad \leq S_j^{\max}\cos\varphi_{j,k} \tag{5.17}$$

The approach used by agent j for computing $P_{G_j,k}$ and $Q_{G_j,k}$ is synthesized in Program 6. Remark that in this program, there is an instruction for adjusting the value of the coefficients K_{P_j} and K_{Q_j}. In our simulations, we assume that this adjustment is done by the agent by learning on-line these parameters. This on-line learning is done by observing changes in the voltage V_{j+2} in the follow up of changes in P_{G_j}

and Q_{G_j}. More specifically, in our simulations, we have computed these values at iteration k by observing two variations of the voltage V_{j+2}: one caused by increasing $P_{G_j,k-1}$ to $P_{G_j,k-1} + 100$ W and the other by increasing $Q_{G_j,k-1}$ to $Q_{G_j,k-1} + 100$ W. On a real system, this would imply that before deciding on the values of $P_{G_j,k}$ and $Q_{G_j,k}$, an agent must be able to take successively two actions and to observe their effects on the system.

Program 6: Logic for agent j to modulate active and reactive power

- Compute the power factor, given current voltage $V_{j+2,k}$

$$\cos\varphi_{j,k} = 1 \qquad \text{if } V_{j+2,k} \leq V^{var} \tag{5.18}$$

$$\cos\varphi_{j,k} = \frac{(\cos\varphi)_{\min} - 1}{V^{ref} - V^{var}}(V_{j+2,k} - V^{var}) + 1 \quad \text{if } V^{var} < V_{j+2,k} < V^{ref} \tag{5.19}$$

$$\cos\varphi_{j,k} = (\cos\varphi)_{\min} \qquad \text{if } V_{j+2,k} \geq V^{ref} \tag{5.20}$$

- Compute allowed rise in voltage

$$\Delta V_{j,k} = V^{ref} - V_{j+2,k} \tag{5.21}$$

- Adjust the value of K_{P_j} and K_{Q_j}.
- Find the amount of active power that will cause a voltage rise equal to $\Delta V_{j,k}$, according to linear model (5.12), with fixed power factor $\cos\varphi_{j,k}$. If necessary, limit this power to satisfy constraints (5.16) and (5.17).

$$P_{G_j,k} = \max\left(0, \min\left(P_{G_j,k}^{\max}, S_j^{\max}\cos\varphi_{j,k}, \frac{\Delta V_{j+2,k} + K_{P_j}P_{G_j,k-1} + K_{Q_j}Q_{G_j,k-1}}{K_{P_j} - K_{Q_j}\frac{\sqrt{1-\cos^2\varphi_{j,k}}}{\cos\varphi_{j,k}}}\right)\right) \tag{5.22}$$

- Compute reactive power

$$Q_{G_j,k} = -\frac{\sqrt{1-\cos^2\varphi_{j,k}}}{\cos\varphi_{j,k}}P_{G_j,k} \tag{5.23}$$

5.4.2 Simulation results

The experimental protocol put in place is the same as in Section 5.3.2. The only change lies in the use of reactive power modulation. To this end, the distributed controller uses Program 6.

Behavior of the test network

Figure 5.4 shows the evolution of voltages for the same changes of $P_{G_j}^{\max}$ as in the previous section. We can see that the voltage variations are quite similar to the case without use of reactive power modulation. There is no change in voltages before the sudden increase of $P_{G_j}^{\max}$ to 7000 W. This was expected since the set of actions taken by the distributed scheme at $t = 0$ corresponds to a stationary point of the system until there is a change in the $P_{G_j}^{\max}$s. After this increase, voltages rise and those at the end of the street slightly overstep the voltage reference V^{ref}, to finally converge to it. However, the difference between the effects of Program 5 and 6 is better understood by looking at Figure 5.5, where the use of reactive power modulation can clearly be observed. This use of reactive power modulation is minor in the first Δt seconds after the increase of $P_{G_j}^{\max}$. It is then more largely put to contribution to finally converge to the distribution of power displayed in Figure 5.6.

Comparison with the centralized control scheme

We will now compare the centralized scheme with the solution the distributed scheme converges to. The graphs comparing voltages, active power and reactive power distributions are given in Figure 5.6. The two voltage profiles are quite similar. The active power distributions are alike, too, with the exception of bus 18 whose active power production is zero. In Section 5.3.2, bus 18 was also exhibiting a singular behavior. This results from the order in which the agents acts, which is the same in this section as in Section 5.3.2. We remark a smaller use of reactive power in the distributed scheme than in the centralized one, but a same trend regarding its use as a function of the house placement in the street. Fixed power factor explains why bus 18 cannot absorb reactive power, as it would be expected. Indeed, the inverter is not producing power and thus cannot produce or absorb reactive power. As can be computed from Table 5.3, the distributed scheme curtails 9.83% more power than the centralized scheme. This is ten times more than without reactive power modulation.

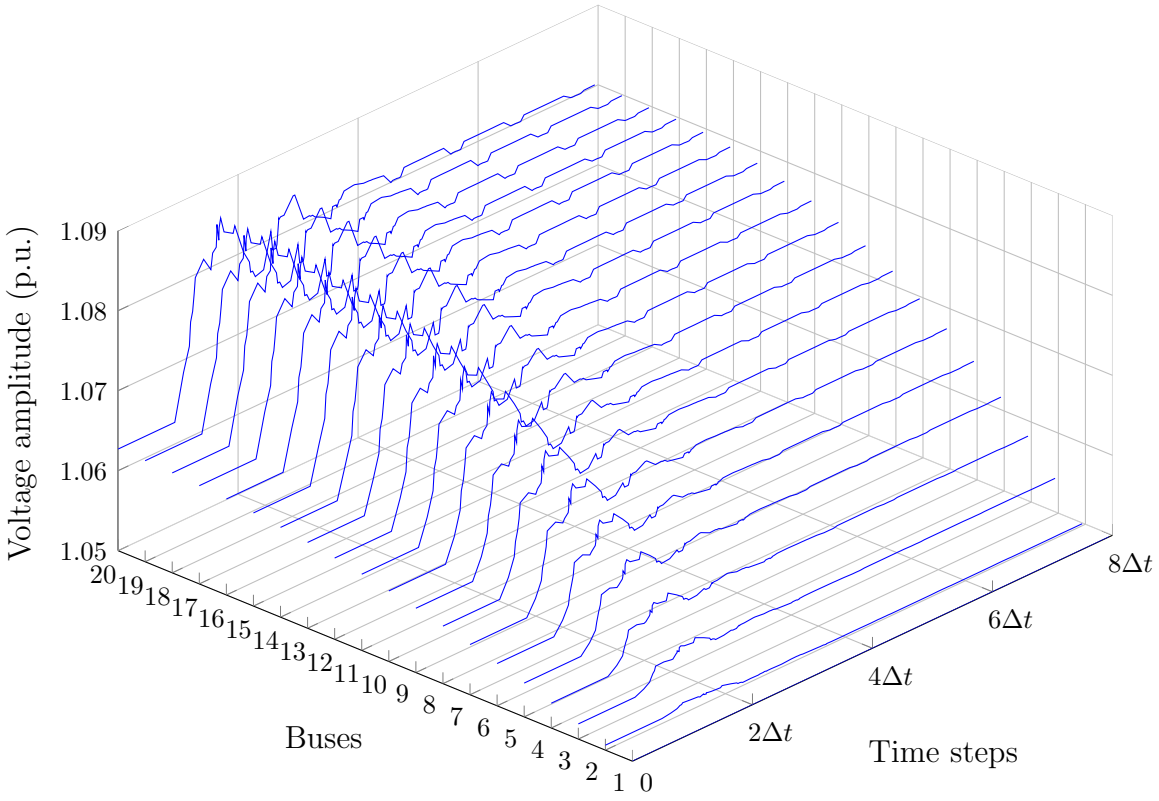

Figure 5.4: Voltage evolution for each bus when $P_{G_j}^{\max}$ $\forall j$ increases from 2000 W to 7000 W at time equal to Δt seconds.

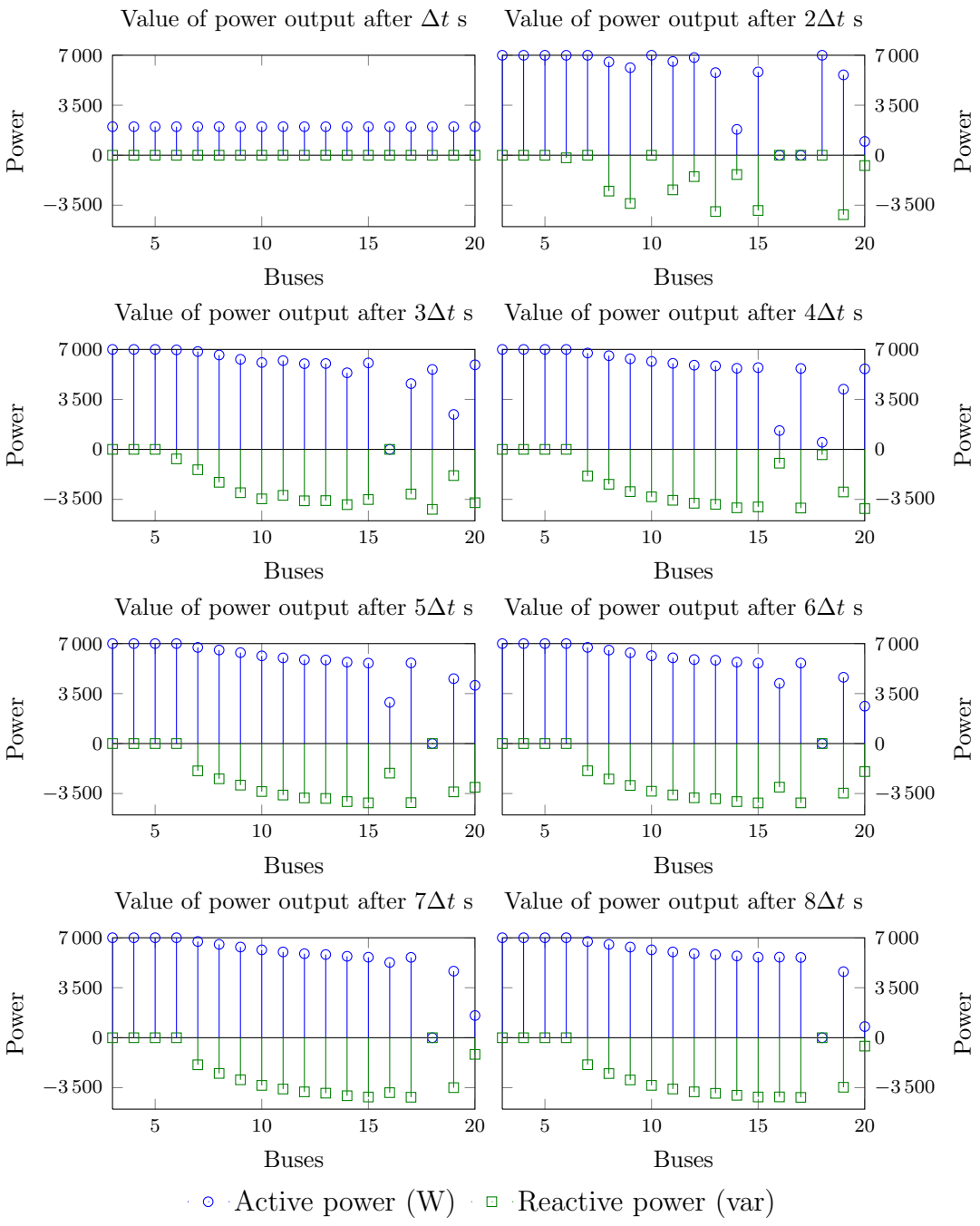

Figure 5.5: Evolution of the power generated by each PV unit.

Nonetheless, when we compare the two distributed schemes with each other, the use of reactive power modulation can save 37% more power, that is 15 715 W.

The same conclusions can be drawn from Table 5.4 when it comes to the amount of electrical energy curtailed during a period of 7 minutes when Δt is equal to 1 minute. The distributed scheme curtails 40% more energy than the centralized one. Again, this percentage could be reduced to its minimuml limit of 9.83% by reducing the time steps. Furthermore, this high percentage of power curtailed must be put into perspective by looking at the amount of reactive energy used. Table 5.5 enlightens us in this regard. Indeed, the centralized scheme uses 56% more reactive energy. As expected, there is a trade-off between the amount of active energy curtailed and the reactive energy used. It could be useful to put a cost on both energy forms and adjust Program 6 parameters to best fit the need of the distribution system operators.

Table 5.3: Comparison between power curtailed in the centralized case and in the distributed case, after convergence.

House	Power curtailed (W)		House	Power curtailed (W)	
	Centralized	Distributed		Centralized	Distributed
1	58.7	0	10	1.4e+03	1.11e+03
2	132	0	11	1.4e+03	1.18e+03
3	263	0	12	1.4e+03	1.28e+03
4	486	0	13	1.4e+03	1.36e+03
5	851	261	14	1.4e+03	1.36e+03
6	1.38e+03	465	15	1.4e+03	1.38e+03
7	1.4e+03	655	16	1.4e+03	7e+03
8	1.4e+03	846	17	1.4e+03	2.38e+03
9	1.4e+03	991	18	5.54e+03	6.22e+03
Total	Centralized	**24114**		Distributed	**26485**

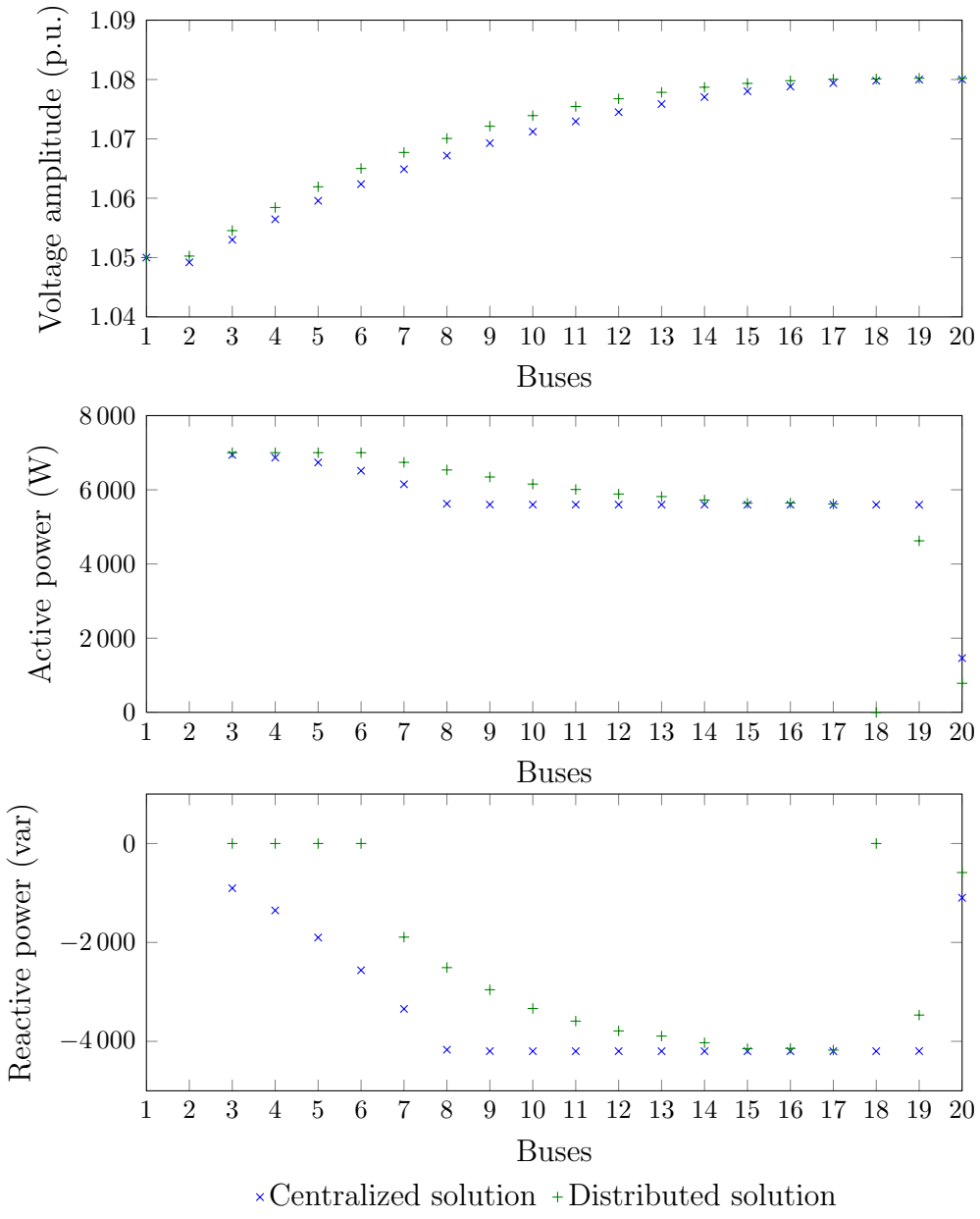

Figure 5.6: Centralized solution and convergence point of the distributed solution when $P_{G_j}^{\max} = 7$ kW $\forall j$.

Table 5.4: Comparison between electrical energy curtailed in the centralized case and in the distributed one over the period $[1\text{ min}, 8\text{ min}]$ when $\Delta t = 1$ min.

House	Energy curtailed (kWh)		House	Energy curtailed (kWh)	
	Centralized	Distributed		Centralized	Distributed
1	0.00588	0.0417	10	0.14	0.135
2	0.0132	0.0417	11	0.14	0.156
3	0.0263	0.0417	12	0.14	0.242
4	0.0486	0.0422	13	0.14	0.166
5	0.0851	0.0615	14	0.14	0.514
6	0.138	0.0861	15	0.14	0.289
7	0.14	0.111	16	0.14	0.523
8	0.14	0.114	17	0.14	0.306
9	0.14	0.128	18	0.554	0.395
Total	Centralized	**2.412**		Distributed	**3.394**

Table 5.5: Comparison between the use of reactive power in the centralized case and in the distributed one over the period $[1\text{ min}, 8\text{ min}]$ when $\Delta t = 1$ min.

House	Reactive energy (kvarh)		House	Reactive energy (kvarh)	
	Centralized	Distributed		Centralized	Distributed
1	0.0903	0	10	0.42	0.338
2	0.135	0	11	0.42	0.383
3	0.19	0	12	0.42	0.358
4	0.256	0.0142	13	0.42	0.398
5	0.334	0.15	14	0.42	0.166
6	0.417	0.245	15	0.42	0.328
7	0.42	0.303	16	0.42	0.0762
8	0.42	0.28	17	0.42	0.322
9	0.42	0.333	18	0.11	0.247
Total	Centralized	**6.1521**		Distributed	**3.9415**

Chapter 6

Conclusions and future work

We have proposed in thesis two types of control schemes, namely centralized and distributed control schemes, for modulating the power injected by PV installations into the low-voltage network so as to mitigate voltage problems. The centralized schemes were based on the resolution of an optimal power flow problem. The distributed schemes were based on simple control logics implemented in the inverters and using only local information. Henceforth, they are less expensive to build than centralized ones. We found out through simulations carried out on a simple test network that the distributed schemes were performing almost as well as the centralized ones, when using as performance metric the amount of energy curtailed on the PV installations. This suggests that they may be a solution of choice for addressing the overvoltage problems caused by PV installations. However, for drawing a firm conclusion about which type of control scheme to implement, one should come with estimates of the costs of building centralized and decentralized schemes as well as estimates of the costs of the energy they will curtail.

Before carrying out this cost analysis, we believe that several other research questions should be first addressed. As a start, we would suggest to further analyze the properties of our distributed control scheme, not only by carrying out additional simulations but also by doing more analytical work. For example, it would be worth identifying under which assumptions the distributed schemes can be proved to converge to a stationary solution. In such a context, bounding the distance between this stationary solution and the solution outputted by a centralized scheme would also be interesting. Another interesting theoretical result would be a bound on the energy curtailed by the scheme over the first T time steps of the trajectory leading

to a stationary solution. Note that we believe that getting such a finite time result may be difficult.

While such a theoretical analysis is certainly extremely interesting and may also suggest new distributed control schemes, we do not expect that it could be carried out on a power system significantly more complex that the simple test system considered in this thesis. Therefore, before implementing these distributed control schemes on a real-life power system, it is also certainly important to simulate their effects on more complex test systems. In particular, we believe that the system that comes atop of the MV/LV transformer should be more carefully modeled than in this manuscript. Indeed, we assumed that it could be represented by an infinite bus system, which is quite questionable.

Finally, it would also be worth studying whether schemes that also control loads at the house level, would not be more interesting to implement than those proposed in this manuscript. Indeed, by modulating flexible loads (e.g., heating or cooling system, electric cars) in a proper way, it should in principle be possible to decrease the amount of energy to be curtailed. However, control schemes exploiting flexible loads are more complex to build. First, they require ad hoc models of the loads that are often difficult to get. Second, the flexible loads add sate variables to the system, which makes the computation of near-optimal control actions much more difficult.

Bibliography

[1] http://eur-lex.europa.eu/LexUriServ/LexUriServ.do?uri=CELEX:32009L0028:EN:NOT. Accessed on May 11th 2013.

[2] M. Braun, T. Stetz, T. Reimann, B. Valov, and G. Arnold. Optimal reactive power supply in distribution networks - technological and economic assessment for pv-systems. In *24th European Photovoltaic Solar Energy Conference, 21-25 September 2009, Hamburg, Germany*, pages 3872 – 3881, 2009.

[3] F. Capitanescu, J.L. Martinez Ramos, P. Panciatici, D. Kirschen, A. Marano Marcolini, L. Platbrood, and L. Wehenkel. State-of-the-art, challenges, and future trends in security constrained optimal power flow. *Electric Power Systems Research*, 81(8):1731 – 1741, 2011.

[4] E. Demirok, D. Sera, R. Teodorescu, P. Rodriguez, and U. Borup. Evaluation of the voltage support strategies for the low voltage grid connected PV generators. In *Energy Conversion Congress and Exposition (ECCE), 2010 IEEE*, pages 710–717, 2010.

[5] M.J. Dolan, E.M. Davidson, I. Kockar, G.W. Ault, and S.D.J. McArthur. Distribution power flow management utilizing an online optimal power flow technique. *IEEE Transactions on Power Systems*, 27(2):790–799, 2012.

[6] S. Frank, I. Steponavice, and S. Rebennack. Optimal power flow: a bibliographic survey I. *Energy Systems*, 3(3):221–258, 2012.

[7] Q. Gemine, E. Karangelos, D. Ernst, and B. Cornélusse. Active network management: planning under uncertainty for exploiting load modulation. In *Proceedings of the 2013 IREP Symposium - Bulk Power Systems Dynamics and Control - IX*, Rethymnon, Crete, Greece, August 2013.

[8] J.D. Glover, M.S. Sarma, and T.J. Overbye. *Power System Analysis and Design*. Cengage Learning, 5th edition, 2011.

[9] C. Gonzalez, J. Geuns, S. Weckx, T. Wijnhoven, P. Vingerhoets, T. De Rybel, and J. Driesen. LV distribution network feeders in belgium and power quality issues due to increasing pv penetration levels. In *Innovative Smart Grid Technologies (ISGT Europe), 2012 3rd IEEE PES International Conference and Exhibition on*, pages 1–8, 2012.

[10] M. Huneault and F.D. Galiana. A survey of the optimal power flow literature. *Power Systems, IEEE Transactions on*, 6(2):762–770, 1991.

[11] P. Kundur, N.J. Balu, and M.G. Lauby. *Power System Stability and Control*. EPRI power system engineering series. McGraw-Hill, 1994.

[12] S.N. Liew and G. Strbac. Maximising penetration of wind generation in existing distribution networks. *IEE Proceedings: Generation, Transmission and Distribution*, 149(3):256–262, 2002.

[13] L.F. Ochoa, C.J. Dent, and G.P. Harrison. Distribution network capacity assessment: Variable DG and active networks. *IEEE Transactions on Power Systems*, 25(1):87–95, 2010.

[14] L.F. Ochoa and G.P. Harrison. Using AC optimal power flow for DG planning and optimisation. In *IEEE PES General Meeting*, 2010.

[15] L.F. Ochoa and G.P. Harrison. Minimizing energy losses: Optimal accommodation and smart operation of renewable distributed generation. *IEEE Transactions on Power Systems*, 26(1):198–205, 2011.

[16] T.A. Short. *Electric Power Distribution Handbook*. Electric power engineering series. Taylor & Francis, 2003.

[17] W.D. Stevenson. *Elements of Power System Analysis*. McGraw-Hill series in electrical engineering: Power and energy. McGraw-Hill, 1982.